NATIONAL WATER RESEARCH INSTITUTE

INSTITUT NATIONAL de RECHERCHE sur les EAUX

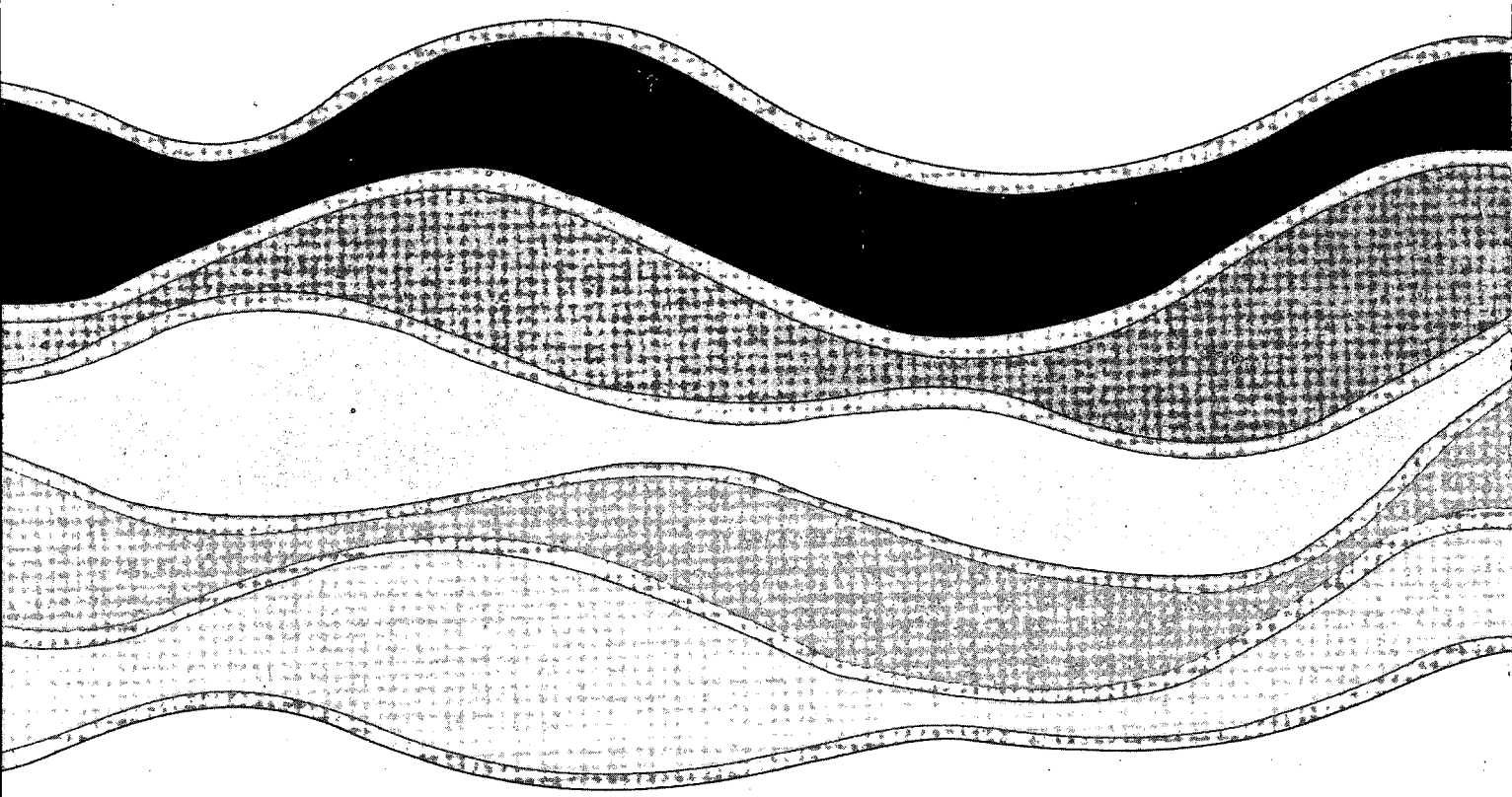

DEEP WATER FIELD EVALUATION OF NDBC/SWADE 3 METER DISCUS DIRECTIONAL BUOY

F. Anctil, M.A. Donelan, G.Z. Forristall
K.E. Steele and Y. Ouellet

NWRI Contribution No. 91-122

Deep Water Field Evaluation of

NDBC/SWADE 3 Meter Discus Directional Buoy.

by

F. Anctil[1], M.A. Donelan[2], G.Z. Forristall[3],

K.E. Steele[4] and Y. Ouellet[1].

submitted to

Journal of Atmospheric and Oceanic Technology

July 1991

---

1 - Université Laval, génie civil, Québec, Québec, CANADA, G1K 7P4

2 - National Water Research Institute, CCIW, Burlington, Ontario, CANADA, L7R 4A6

3 - Shell Development Company, Houston, Texas, U.S.A., 77001

4 - National Data Buoy Center, Stennis Space Center, Mississippi, U.S.A., 39529

MANAGEMENT PERSPECTIVE

The U.S. National Data Buoy Centre (NDBC) routinely measures wave directional properties using meteorological buoys of 3 metres diameter. These relatively small buoys have a proven track record, which led to their selection as the principal surface stations in the large international Surface Waves Dynamics Experiment (SWADE). Substantial modification to the design and payload of these buoys was required for SWADE, and consequently a field evaluation of the new design in deep water was deemed necessary.

This paper provides a comparative analysis of wave spectra, directional spectra and statistics obtained from one of these NDBC/SWADE buoys against corresponding information from an oil production platform ("Bullwinkle") in the Gulf of Mexico . The platform stands in 415 m of water and provided a truly deep water reference. The comparison indicates that the modified NDBC/SWADE buoys are in agreement with the Bullwinkle platform within the expected variability associated with sampling and their 1 km separation. These results provided the necessary validation of the new NDBC/SWADE design prior to its use in the Surface Wave Dynamics Experiment.

SOMMAIRE À L'INTENTION DE LA DIRECTION

Le U.S. National Data Buoy Centre (NDBC) mesure systématiquement les propriétés directionnelles des vagues au moyen de bouées météorologiques de 3 mètres de diamètre. La bonne performance de ces bouées assez petites étant bien établie, elles ont été choisies comme principales stations de surface dans le cadre de l'importante expérience internationale SWADE (Surface Waves Dynamics Experiment). Aux fins de cette expérience, il a fallu modifier de façon importante la conception et le poids utile en charge de ces bouées, et il a donc été jugé nécessaire d'effectuer une évaluation sur le terrain en eau profonde de la nouvelle conception utilisée.

Le présent article offre une analyse comparative des spectres des vagues, des spectres directionnels et des statistiques provenant d'une de ces bouées NDBC/SWADE par rapport à des informations correspondantes provenant d'une plate-forme d'exploitation pétrolière ("Bullwinkle") dans le golfe du Mexique. La plate-forme se trouve par 415 m de profondeur et constitue une bonne station de référence en eau profonde. D'après les données de comparaison, les bouées modifiées NDBC/SWADE sont en accord avec la plate-forme Bullwinkle, compte tenu de la variabilité prévue associée à l'échantillonnage et de la distance de 1 km devant les séparer les unes des autres. Ces résultats fournissent la validation nécessaire de la nouvelle conception de la bouée NDBC/SWADE avant qu'elle soit utilisée dans le cadre de l'expérience SWADE.

ABSTRACT

This paper presents the results of an experiment designed to assess the directional spectrum resolution qualities of the pitch-roll-heave NDBC/SWADE 3 meter discus wave directional buoy, in deep water conditions. Wave frequency spectra and wave directional spectra measured by the buoy, moored in about 415 m water depth, are compared to similar measurements obtained from a wavestaff and a bi-axial current meter fixed to the nearby Bullwinkle platform (Gulf of Mexico). Both buoy and platform equipment operated simultaneously from 0000 GMT 29 May 1989 to 0100 GMT 24 June 1989.

The analysis revealed that the buoy surface displacement energy spectra (estimated from heave acceleration) agree well with the platform spectra. Comparison of mean direction and directional width parameters is favourable considering the large variability of those estimators. Discrepancies are reduced when records of significant wave height less than 1 meter are eliminated.

RÉSUMÉ

Le présent article présente les résultats d'une expérience visant à évaluer les qualités de résolution du spectre de direction d'une bouée NDBC/SWADE (disque de 3 mètres) qui mesure le tangage, le roulis et le pilonnement en eau profonde. Les spectres de la fréquence des vagues et les spectres de la direction des vagues mesurés par la bouée, mouillée par environ 415 m de profondeur, sont comparés à des mesures similaires d'un houlographe et d'un courantomètre biaxial fixés à la plate-forme Bullwinkle se trouvant à proximité (golfe du Mexique). La bouée et les appareils de la plate-forme ont fonctionné simultanément entre 0000 GMT le 29 mai 1989 jusqu'à 0100 GMT le 24 juin 1989.

L'analyse a montré que les spectres d'énergie du déplacement en surface de la bouée (évaluée à partir d'une accélération du pilonnement) concordent bien avec les spectres mesurés à partir de la plate-forme. La comparaison des paramètres de la direction moyenne et de la largeur de la direction est favorable, compte tenu de la grande variabilité de ces estimateurs. Les écarts sont réduits lorsque l'on élimine des mentions de la hauteur caractéristique des vagues inférieures à 1 mètre.

1 INTRODUCTION

The Surface Wave Dynamics Experiment (SWADE), Weller *et al.* (1991), is concerned primarily with the evolution of the directional wave spectrum in both time and space, improved understanding of wind forcing and wave dissipation, the effect of waves on air-sea coupling mechanisms and the radar response of the surface. To achieve these objectives, an experimental plan using moored buoys and aircraft was developed. The task of continuously monitoring the waves rests primarily with NDBC/SWADE 3 meter discus directional buoys. This paper presents the results of an experiment, prior to SWADE, designed to assess the directional spectrum resolution qualities of the pitch-roll-heave NDBC/SWADE 3 meter discus directional buoys, in deep water conditions. Note that some similarities exist with the Wave Direction Measurement Calibration Project (WADIC), Allender *et al.* (1989), which compared the directional resolution of six directional buoys: Marex, Norwave, Wadibuoy, Wavec, Wavescan, and Wavetrack.

The next section describes the experimental site and the instrumentation used. Section 3 summarizes the data analysis methods used to parameterize the non-directional and directional sea states and gives an overview of the variability confidence limits of the main parameters. Specific adjustments to the NDBC/SWADE buoy measurements are dealt with in section 4. A comparison of wave directional data from the buoy (derived from data sent to shore via satellite) to corresponding data from the platform is described in section 5. A more detailed intercomparison is performed in section 6, using the available time series from both systems, including the environmental conditions for that period. Finally the last section states the main conclusions derived from this experiment.

2 SITE AND INSTRUMENTATION DESCRIPTION

The offshore oil production platform called "Bullwinkle" provides an excellent site for deep water evaluation of a buoy: it is the tallest man made structure in the ocean (Digre *et al.* 1989), in water depth of 415 m, and it is equipped for the directional estimation of sea states (Swanson and Baxter, 1989). Bullwinkle is located in the Gulf of Mexico (27°52'59"N and 90°54'05"W) on a bed slope of 2.2%. The nearest coast is about 120 km north, and New Orleans is 240 km to the north-north-east. The buoy mooring site is 1.5 km east-south-east of the platform (27°52'36"N and 90°53'13"W). Both buoy and platform equipment operated simultaneously from 0000 GMT 29 May 1989 to 0100 GMT 24 June 1989, but the buoy's onboard time series recording system stopped at 0400 GMT 7 June 1989, while the buoy's satellite transmission kept working. The present comparison is, in fact, performed with three data sets: the Bullwinkle platform's time series, the buoy's time series recorded on board (hereafter identified as NWRI) and the buoy's spectral estimates transmitted to shore (hereafter called NDBC).

The platform instrumentation used in this comparison was a Marsh-McBirney 551 bi-axial current meter, located 6 m (20 ft) below mean water level, and a 30 m (100 ft) wave staff, Baylor's 19595-1100. Data were sampled at 1 Hz for a period of 1 hour, beginning and ending at the hour, every 3 hours.

The NDBC/SWADE 3 meter discus directional buoy instrumentation list was as follows: one directional wave measurement device (that outputs vertical acceleration, pitch and roll), Datawell's Hippy 40 Mark II; one tri-axial fluxgate magnetometer, Develco's 9200; three orthogonaly mounted accelerometers, two Sunstrund's KA1100 and one KA1400; and one twin propeller anemometer, Young's K-Gill 35351. Two additional instruments were located along the mooring line at about 15 m below mean water level: one bi-axial current meter, Neil Brown's Smart Acoustic; and one tension gage, Metrox's TL101-10K. The major difference with NDBC buoy standard structural configuration is the addition of a 2 m^2

wind vane to one of the mast legs, so that the buoy is forced to orient itself according to the wind, thereby essentially eliminating the difficulty of proper exposure of meteorological instruments and providing some directional stability. All the main buoy instruments were continuously sampled at 1 Hz by a LOPACS computer and the outputs were stored on an onboard optical disk recording system; the current meter and the tension gage measurements were stored within those instruments and consisted respectively of 5 minute averages every 10 minutes and of 4 minute averages every 4 minutes.

During the whole experiment, all the standard equipment of a NDBC 3 meter discus directional buoy (Steele *et al.* 1990) functioned properly, which implies that the "on board" processing system was operational and transmitted directional wave spectrum information to shore, via satellite. The sampling rate of the "on board" system was 2 Hz, and the data collection lasted roughly 20 minutes every hour.

3 DATA ANALYSIS

Spectral analysis is based on the assumption of an ergodic gaussian process with zero mean. Ergodicity assures that a record is representative of the same process from start to end, and that it is statistically equivalent to any other record from an ensemble collected in that period and area. There is no simple way to assess that condition because of the difficulty of collecting a true ensemble of wave records for a prescribed sea state, due to wind variability in time and space. Howerver, measurement constancy over short periods is expected, so in short records stationarity is usually assumed and even ergodicity. Non normality of a signal reflects the presence of some non-linear components, for example a surface displacement signal is positively skewed when crests are higher than troughs, a phenomenon usually associated with shallow water or strong wind forcing. In all cases, some divergence from the ideal record is inevitable; the quality of the analysis, especially in a probabilistic sense, may then suffer.

3.1 Non-directional parameters

Wave height is first characterized by the root-mean-square surface displacement about its mean η_{rms},

$$\eta_{rms}^2 = \sigma_\eta^2 = E[\eta_i^2] = \int_{-\infty}^{\infty} \eta_i^2 \, p(\eta) \, d\eta \ , \qquad (1)$$

in which η_i is the detrended surface displacement signal, σ_η^2 its variance (mean square value), E[ ] the expected value operator and p( ) the probaibility density operator. Frequency domain analysis also leads to η_{rms},

$$\eta_{rms}^2 = m_0 = \int_0^{f_c} f^0 \, S_{\eta\eta}(f) \, df \ . \qquad (2)$$

using the spectral moment of order zero, m_0, which is the integral of the surface displacement frequency spectrum $S_{\eta\eta}(f)$, a representation of the variance of the signal per frequency band.

Several estimators have been proposed for the wave period, three of them are used here: peak period T_p,

$$T_p = \frac{1}{f_p} \ , \qquad (3)$$

where f_p is the frequency of maximum $S_{\eta\eta}$, and two mean periods T_{01} and T_{02}, which are combinations of m^{th}-order spectral moments,

$$T_{01} = \frac{m_0}{m_1} \ , \qquad (4)$$

$$T_{02} = \left(\frac{m_0}{m_2}\right)^{0.5} \ . \qquad (5)$$

Surface displacement records can also be analyzed in the time domain, via mean level upcrossing. Each wave is then defined by two successive upcrossings at the mean level.

Wave periods T are the elapsed time between each crossing, and wave heights H are the differences of the highest crests and lowest troughs between each crossing. To compensate for errors caused by discretization, the time at each crossing is linearly interpolated and signal maxima and minima are estimated via parabolic interpolations based on 3 points. Various probabilistic parameters are deduced from height and period time series: mean height $\overline{H}$ and mean period $\overline{T}$ are average values; $H_{1/3}$ is the mean value of the highest 1/3 waves and $T_{1/3}$ the average value of the corresponding periods; $H_{1/10}$ and $T_{1/10}$ are obtained the same way but for the highest 1/10 waves; H_{max} is the highest wave and T_{max} its period.

$\overline{H}$, $H_{1/3}$, and $H_{1/10}$ are all statistically related by a height probability distribution. The Rayleigh distribution (Longuet-Higgins, 1952) is usually taken as a first order description of wave height statistics, assuming narrow band spectra, and that peak values are statistically independant. In the same manner, root-mean-square surface displacement η_{rms} can also be given a probabilistic meaning (Goda 1985):

$$4\,\eta_{rms} = 4\,m_0^{0.5} = H_s\,. \qquad (6)$$

It can also be shown that the zero upcrossing mean period $\overline{T}$ of narrow-band spectra (Rayleigh) leads to the same value as T_{02} (Goda 1985).

Since the wave height distribution varies from record to record, a spectral width parameter ε has been proposed (Cartwright and Longuet-Higgins, 1956):

$$\varepsilon = \left(\frac{m_0\,m_4 - m_2^2}{m_0\,m_4}\right)^{0.5} \cong \left[1 - \left(\frac{N_0}{N_1}\right)^2\right]^{0.5}. \qquad (7)$$

Its evaluation is based on spectral moments, or it can be approximated from N_0 and N_1, which are respectively the number of zero upcrossings and the number of maxima per record. For the Rayleigh distribution ε equals 0. Even if most sea waves (ε ranging form 0.4 to 0.8

) do not exactly follow the Rayleigh distribution, Ochi (1982) showed that the significant wave height overestimation is usually contained between 1% and 8%.

Wave period distribution is estimated and compared to the theoretical formulation proposed by Longuet-Higgins (1983), which is a function of

$$\nu = \left(\frac{m_0 m_2 - m_1^2}{m_1^2} \right)^{0.5}, \qquad (8)$$

a parameter also describing the width of a spectrum. Finally, wave height and period joint frequency distributions and lengths of runs of high waves (see for exemple Goda (1985)) are compared. They respectively give a quick view of the correlation between height and period and of the extent of wave grouping.

3.2 Directional parameters

Three signals, surface displacement with two orthogonal slopes (η, x-eastward and y-northward) or surface displacement with two orthogonal current velocities (η, u-eastward and v-northward), yield a coarse view of the actual directional spectrum. The lack of complete spatial information has to be compensated in some way, usually by the use of a model describing the direction distribution $D_f(\theta)$, or else by the acceptance of a limited number of directional parameters for the description of wave directionality. The latter approach is selected here for its simplicity and straightforwardness, and its general use as a standard procedure for the routine analysis of sea wave data.

Kuik *et al.* (1988) proposed a method that yields four model-free parameters per frequency: the mean direction θ_0, the directional width σ, the skewness γ and the kurtosis δ of the directional energy distribution,

$$D_f(\theta) = \frac{F(f,\theta)}{S_{\eta\eta}(f)} , \qquad (9)$$

where $F(f,\theta)$ and $S_{\eta\eta}(f)$ respectively are the directional spectrum and the frequency spectrum. Each parameter is expressed analytically in terms of the four Fourier coefficients (derived from the auto-, co- and quadspectra of the three wave related signals) used by Longuet-Higgins *et al.* (1963) to form a truncated Fourier series approximating the direction distribution at each frequency. For the surface displacement and slopes triplet, the Fourier coefficients take the form:

$$a_1(f) = \int_0^{2\pi} \cos(\theta) D_f(\theta)\, d\theta = \frac{Q_{\eta x}(f)}{k(f)\, S_{\eta\eta}(f)} , \qquad (10)$$

$$b_1(f) = \int_0^{2\pi} \sin(\theta) D_f(\theta)\, d\theta = \frac{Q_{\eta y}(f)}{k(f)\, S_{\eta\eta}(f)} , \qquad (11)$$

$$a_2(f) = \int_0^{2\pi} \cos(2\theta) D_f(\theta)\, d\theta = \frac{S_{xx}(f) - S_{yy}(f)}{k(f)^2\, S_{\eta\eta}(f)} , \qquad (12)$$

$$b_2(f) = \int_0^{2\pi} \sin(2\theta) D_f(\theta)\, d\theta = \frac{2C_{xy}(f)}{k(f)^2\, S_{\eta\eta}(f)} , \qquad (13)$$

where S represents the autospectra, C the cospectra and Q the quadspectra, and k is the wavenumber. For the surface displacement and current meter triplet, x and y are replaced by u and v, respectively, and $Q_{\eta x}$ and $Q_{\eta y}$ are replaced by the corresponding cospectra.

The vectorial average of the directional distribution θ_0, measured counterclockwise from the east to the direction of propagation, or more simply the mean direction, is a function of the first two Fourier series coefficients,

$$\theta_0 = \tan^{-1}(b_1, a_1) . \qquad (14)$$

The other parameters are based on the second, third and fourth order circular moments μ_{ij},

$$\mu_{02} = 2(1 - \alpha_1), \tag{15}$$

$$\mu_{20} = (1 - \alpha_2)/2, \tag{16}$$

$$\mu_{12} = 2\beta_1 - \beta_2 = -\beta_2, \tag{17}$$

$$\mu_{04} = 6 - 8\alpha_1 + 2\alpha_2, \tag{18}$$

in which α_1, α_2, β_1, β_2 are centered Fourier coefficients given by:

$$\alpha_1 = \int_0^{2\pi} \cos(\theta - \theta_0) D_f(\theta)\, d\theta = a_1 \cos\theta_0 + b_1 \sin\theta_0 = (a_1^2 + b_1^2)^{0.5}, \tag{19}$$

$$\alpha_2 = \int_0^{2\pi} \cos[2(\theta - \theta_0)] D_f(\theta)\, d\theta = a_2 \cos(2\theta_0) + b_2 \sin(2\theta_0), \tag{20}$$

$$\beta_1 = \int_0^{2\pi} \sin(\theta - \theta_0) D_f(\theta)\, d\theta = b_1 \cos\theta_0 - a_1 \sin\theta_0, \tag{21}$$

$$\beta_2 = \int_0^{2\pi} \sin[2(\theta - \theta_0)] D_f(\theta)\, d\theta = b_2 \cos(2\theta_0) - a_2 \sin(2\theta_0), \tag{22}$$

where $\beta_1 = 0$ by virtue of (14). Since there are two different second order moments (μ_{02} and μ_{20}), two complete sets of parameters can be defined. Kuik *et al.* (1988) selected the following three parameters on the basis of the criterion that they react more closely to similar parameters based on linear moments:

$$\sigma = \mu_{02}^{0.5} = [2(1 - \alpha_1)]^{0.5} , \tag{23}$$

$$\gamma = \frac{\mu_{12}}{\mu_{20}^{1.5}} = \frac{-\beta_2}{[(1 - \alpha_2)/2]^{1.5}} , \tag{24}$$

$$\delta = \frac{\mu_{04}}{\mu_{02}^{2}} = \frac{6 - 8\alpha_1 + 2\alpha_2}{[2(1 - \alpha_2)]^{2}} . \tag{25}$$

3.3 Sampling variability confidence limits

Each spectrum estimator has a certain level of precision that can be improved only by increasing the set of points used to evaluate it. Sampling variability, approximately follows a chi-square χ^2 distribution with ρ degrees of freedom (roughly the number of points used to compute each estimator). Limits to bound the true spectrum estimators $\hat{S}_{\eta\eta}(f)$ are evaluted, for a $(1 - \alpha)$ probability confidence interval, using:

$$P\left(\frac{\rho}{\chi^2_{\rho:\frac{\alpha}{2}}} S_{\eta\eta}(f) \le \hat{S}_{\eta\eta}(f) \le \frac{\rho}{\chi^2_{\rho:1-\frac{\alpha}{2}}} S_{\eta\eta}(f) \right) = (1 - \alpha) , \tag{26}$$

where $S_{\eta\eta}(f)$ are the estimated spectral values.

Since significant wave height H_s is derived from spectrum estimators, a similar approach is used to determine its sampling variability. Even if all the points of a record are used to estimate H_s, its total degree of freedom TDF is less because only independent points are retained. Donelan and Pierson (1983) showed that the TDF is approximated by:

$$\text{TDF} \equiv \rho \frac{[\Sigma S_{\eta\eta}(f)]^2}{\Sigma[S_{\eta\eta}(f)]^2} , \tag{27}$$

and that for large TDF values, $\hat{H}_s$ 90% confidence intervals are:

$$P\left(\left(10^{-(\text{TDF})^{-0.5}}\right)^{0.5} H_s \le \hat{H}_s \le \left(10^{+(\text{TDF})^{-0.5}}\right)^{0.5} H_s \right) = 0.90 . \tag{28}$$

Based on the work of Long (1980) and Borgman *et al.* (1982), Kuik *et al.* (1988) rewrote root-mean-square error formulations of the mean direction θ_0 and of the directional width σ, using the directional width σ and kurtosis δ values:

$$\mathrm{rms}(\theta_0) = \rho^{0.5} \frac{\sigma}{\left(1 - \frac{\sigma^2}{2}\right)} \left(1 - \frac{\delta\sigma^2}{4}\right)^{0.5}, \qquad (29)$$

$$\mathrm{rms}(\sigma) \cong \rho^{0.5} \frac{\sigma(\delta - 1)^{0.5}}{2}, \qquad (30)$$

in which ρ is the degree of freedom value for each frequency band. Kuik *et al.* (1988) have not given any expression for the skewness or the kurtosis error due to sampling variability, but they have performed a Monte-Carlo simulation to assess that question and have determined the following root-mean-square error margins: 5° - 10° for mean direction, 10% - 15% for direction width, 30% - 50% for skewness and 25% - 100% for kurtosis.

4 ADJUSTMENT OF THE BUOY MEASUREMENTS

The design of a hull-mooring can prevent the hull acting as a perfect wave follower. On site verification of that aspect is extremely difficult, so it is usually performed after the fact via comparison with a reference data base or theoretically, assuming sea state linearity. Comparison of buoy data with linear theory indicated that corrections to the amplitude and the phase of the slopes were necessary and that at low frequencies (< 0.05 Hz) noise had to be considered in the acceleration signals. This is well known (Steele *et al.* 1985 and 1990).

It should also be stressed that precise calibration and a thorough knowledge of the buoy's instrumentation response are necessary to take full advantage of the buoy's measurement capacity.

4.1 Influence of the mooring line pull

Tension measurements of the mooring line were carried to detect possible influence on the buoy motions. During the 9 day overlap when all systems were fully operational, the four minute mean tension varied from 337 kg to 885 kg, with a mean of 582 kg and a standard deviation of 91 kg (see Figure 5). The reserve buoyancy of the buoy is 4900 kg, so these tensions do not seriously inhibit the heave response of the buoy. The submerged weight of the mooring line is estimated to be 550 kg.

4.2 Heave acceleration double integration

The Hippy 40 Mark II accelerometer produces an analog of the earth-vertical component of buoy acceleration that includes some electronic noise and, as it is sampled, digitization noise. Unless the noise in the acceleration time series is somehow first removed, it will be increasingly amplified in the conversion of acceleration spectra to displacement spectra, as frequency decreases. We note that, in the absence of low frequency waves, the acceleration spectrum is level at low frequencies, suggesting that the noise (at the low end of the spectrum, at least) is white. We assume that white noise is added to all frequencies and used the band centered at 0.02 Hz as indicator of the level of noise. The integration procedure to obtain displacement from acceleration is the following. The acceleration time series is first Fourier transformed. Secondly, the magnitude of each complex Fourier coefficient is reduced in a mean square sense by the value at 0.02 Hz — any resulting negative values are set to zero — the phase remaining unaltered. Then, each Fourier coefficient is multiplied by $(i\omega)^{-2}$ to obtain the equivalent displacement Fourier coefficient. Finally, an inverse Fourier transform is performed, which yields the displacement time series.

Figure 1 compares typical buoy displacement spectra, computed from the noise-corrected acceleration samples, to platform displacement spectra.

The buoy high frequency response is limited by its size. However, in the frequency range of interest (up to 0.5 Hz), the hull mooring response in heave does not deviate from unity by more than a few percent at most. It appears that the hull dynamical response compensates its spatial filtering effect over that frequency range (see Kim 1966, Stewart 1977). The buoy-derived spectra show a high frequency decay as ω^{-4}. This is the established behaviour of the equilibrium range of wind sea spectra (Forristal 1981, Kahma 1981, Donelan *et al.* 1985). On the other hand, the platform spectra show a slower decay above 0.3 Hz. This appears to be related to electronic noise in the measurements of surface elevation from the platform.

4.3 Phase shift adjustment

To detect any anomalies in the buoy wave following capacities, a simple test can be performed, assuming a linear sea state: wavenumbers estimated from the spectra of the three buoy signals should equal the theoretical ones k_{th}, their ratio R_h thus leading to a value of one:

$$R_h(f) = \frac{\left(\dfrac{S_{xx}(f) + S_{yy}(f)}{S_{\eta\eta}(f)}\right)^{0.5}}{k_{th}(f)} \quad . \qquad (32)$$

Any divergence from a unit value shows that the wave field is non-linear, or that the buoy heave and slope motions do not coincide exactly with wave motions, or that Doppler shifts, introduced by currents, are significant. Theoretical phase differences between surface displacement and slopes is $\pi/2$ for a linear wave field, which leads to imaginary only cross-spectra. Any artificial phase shift Φ_h between surface displacement and slopes is determined

by removing $\pi/2$ from the overall phase differences estimated from the measured cross spectra of slopes and displacement.

Measured spectra and cross spectra showing divergence from the theoretical wavenumbers and phase differences, indicate imperfections in the following ability of the buoy when the wave field is not steep and there is little current (Figure 2). The mooring system is probably the main source of restriction in the free motion of the buoy, but hull and tripod design may also contribute to it. Following an idea developed by Steele *et al.* (1985 and 1990), the measured spectra and cross spectra were scaled to fit linear theory, in order to compensate for the buoy discrepancies.

Assuming that the surface displacement variance is adequately estimated by the buoy (comparison with platform data shows that the surface displacement variance error is small), the wavenumber ratio R_h was used to correct the slope variances. Secondly, cross spectral energy was redistributed, using the deduced phase shifts Φ_h between surface displacement and slopes. A weighted average was performed to assure a unique phase shift per frequency, valid for both slopes. Such a procedure is certainly incorrect for non linear cases, like highly forced waves, shallow water or strong current conditions, but seems realistic for most sea states, especially in deep water.

Figure 2 shows the overall mean values of the wavenumber ratios R_h and the deduced phase shifts Φ_h for this experiment, as determined from the satellite transmission of NDBC "on board" analysis. The mean wavenumber ratio value is around 0.45 for most of the frequencies with significant wave energy, and the mean phase shift oscillates around -35 deg for the same frequencies. No significant energy was observed below 0.11 Hz in this experiment.

5 GENERAL RESULTS

For the whole experiment (0000 GMT 29 May 1989 to 0100 GMT 24 June 1989), the standard NDBC "on board" directional wave analysis system was operational and transmitting results to shore. That data set can then be compared to the measurements performed on the Bullwinkle platform, which gives 195 simultaneous records. It is however difficult to simulate exactly the computation performed on the buoy using platform data; for instance the sampling rate used is 2 Hz instead of 1 Hz for the platform measurements, so comparison here will be limited to general parameters, namely: significant wave height, peak period, mean direction at the peak and corresponding directional width angle.

The buoy "on board" analysis (Steele *et al.* 1990) is performed on 20 minutes of data, starting at 22 minutes after the hour. It is divided in 100 s windowed blocks, overlapped by 50 s. The surface displacement spectral estimators are averages for frequencies ranging from 0.01 to 0.40 Hz, in steps of 0.01 Hz, while the co- and quad-spectra are averages for frequencies ranging from 0.03 to 0.35 Hz, also in steps of 0.01 Hz. Each estimator is produced with approximately 24 degrees of freedom.

Platform spectral computations is based on 19.2 minutes of data, starting at 22 minutes after the hour. They are conducted using a Welch (1967) type approach, *i.e.* estimators are averaged over 17 blocks of 128 s in length, overlapped by 50%, which leads to 28 degrees of freedom. Each block is detrended and windowed beforehand. A 4-term Blackman-Harris window (Harris, 1978) is selected here not only because of its general performance, but also because it limits the correlation of two successive 50% overlapped blocks to only 3.8%.

Figure 3 presents scatter plots of platform vs buoy measurements of significant wave height, peak period, mean direction at the peak, and directional width at the peak. It can be seen that significant wave height measurements compared favorably, but that the variability

of the three other parameters is quite large. In fact, it seems that the directional width is biased, giving larger values for the platform than for the buoy. Note that similar variability was found in the WADIC intercomparison project (Allender *et al.* 1989). When cases with platform significant wave height less than 1 meter are removed, some of the peak period and mean direction variability is eliminated (Figure 4).

6 DETAILED ANALYSIS

From 0000 GMT 29 May 1989 to 0400 GMT 7 June 1989, time series are available from NWRI (buoy) and Bullwinkle (platform) measurement systems. Only simultaneous data from both sets are used for comparison, which leads to 68 1-hour records (3600 values starting at the hour, every 3 hours). Spectral computation is conducted identically on both data sets (as described in the previous section for the platform) except that now the data are divided into 55 blocks of 128 s in length, leading to 90 degrees of freedom. Time domain analysis is carried out via mean level upcrossing, after each record has been detrended. All computations were performed with the MatLab program and subroutines (The MatWorks, 1988).

6.1 Environmental conditions

Some technical difficulties prevented the normal functioning of the upper K-Gill anemometer, so only the average horizontal wind speed is estimated. The wind direction (coming from) is determined from the buoy orientation, a large vane keeping the buoy and the anemometer facing the wind in all but light winds. Figure 5 summarizes the wind conditions over 20 minute periods (averaging time following Pierson (1983)). Most mean speeds oscillate between 4 and 8 m/s, while the wind direction turns slowly from north-east to south-west.

The buoy's current meter measurements are also plotted on Figure 5. These show substantial westward current with a diurnal tide superimposed; maximum velocities are around 0.6 m/s. Water temperature rises gradually from 26.5 to 28 °C.

Tension measurements of the mooring line (average over an hour) are also presented in Figure 5. It appears that tension is related primarily to current fluctuations.

6.2 Non directional parameters

The root-mean-square deviations of platform and buoy surface displacement records are compared in Figure 6, where we can see that agreement between the data sets is excellent. Note that the double integration of the buoy's acceleration assumes that its phases are similar to the phases of the actual water surface that forces the movements of the buoy. The platform wave staff is a pure Eulerian sensor (fixed), while the buoy is quasi-Lagrangian (free-floating but tethered). The type of sensor has no effect on the measured energy level of the resulting surface displacement signal, but it may affect its shape, particularly for steep waves. For instance, Longuet-Higgins (1986) showed that a Lagrangian sensor may overestimate the wave period, when the "Stokes drift" of high waves tends to carry the buoy forward — it is dragged back by the mooring during intervals of lower waves. This phenomenon explains some of the discrepancies depicted here.

The buoy (Figure 6) shows very little surface displacement skewness while the platform skewnesses are generally positive and range up to 0.4. Similar results have been reported by James (1986) who used second-order theory to demonstrate that a free floating buoys will be unaffected by the second harmonic of the surface displacement. The same conclusion holds for tethered buoys to some degree, but in that case the mooring system may allow the measurements of some second order components. Figure 6, on the other hand, shows no relation between platform and buoy kurtosis.

From the spectral analysis, four parameters are presented here (Figure 7): significant wave height H_s, mean period T_{02}, peak period T_p and spectral width ε. The significant wave height H_s is deduced from the root-mean-square deviation of the surface displacement and so exhibits the same relation; however when the 90% confidence limits are compared, there are only 28 cases out of 68 which ovelap. The 1.5 km distance between the buoy and the platform is large enough for each system to be subjected to slightly different sea states, and thus increase the variability. The good agreement between sets is confirmed by the unbiassed scatter plot. The peak period T_p also shows no bias, but a larger variability. The mean period T_{02} (and T_{01}, not shown here) is biased toward the buoy (quasi-Lagrangian measurements). Finally, the spectral width ε is well correlated, but slightly biased.

Spectral analysis results are confirmed by mean level upcrossing parameters (Figure 8): wave heights are similar, and buoy mean periods are longer than the platform ones.

Figures 9 to 12 show the height, period and surface displacement probability density distributions, the normalised height and period joint frequency distribution and the occurence probability of the length of run of high waves. These Figures compare buoy and platform surface displacement measurements for two typical events (1500 GMT 2 June 1989 and 1200 GMT 3 June 1989) characterized by a peak period of about 7 s and a significant wave height repectively of 1.1 m and 0.9 m — the second event has a second peak at 4.5 s (see Figure 1). There is excellent agreement between data sets, but the wave period distributions do not always match the theoretical distribution.

6.3 Directional parameters

To increase the number of estimates, the comparison of directional parameters is performed not only with values corresponding to the spectral energy peak, but also with the values of the three frequency bands (Δf = 1/128 Hz) preceeding the peak and the three

following it, thus giving 7 estimators covering a band of about 0.055 Hz centered at the peak. A first look at Figure 13 is not very encouraging: some mean directions agree but there is considerable scatter; directional width variability is large, directional skewness seems unrelated; and many buoy kurtosis estimates are much larger than the platform values. However sampling variability of directional parameters is large, so if we take that factor into account when comparing data sets, 44 mean direction cases and 48 directional width cases out of 68 are within each other's 90% confidence limits. For records with buoy significant wave height greater than 1 meter, mean direction and spread discrepancies are greatly reduced and skewness agreement is also improved (Figure 14).

Figures 15 and 16 present mean direction and directional width as a function of frequency, for the two events considered earlier, where (a) is the buoy and (b) the platform. Here, power spectra (dotted line) are normalized so that the peak value is 360. The agreement is good, even the different mean directions of swell and wind sea (Figure 16) are similarly measured by both systems. Note that for low frequency the wave energy is too small to lead to any relevant directional information, and that the platform mean direction values are noisy beyond about 0.35 Hz, probably because of the rapid attenuation of the current with depth at these wavenumbers and higher.

The comparison between buoy and platform described have contained some variability associated with the 1.5 km separation of the two measuring systems. An internal check of the buoy mean direction tracking stability is possible under the assumption that the shortest waves quickly adjust to the wind direction at these long fetches. In Figure 17 we compare the mean wave direction from the buoy for f = 0.35 Hz with the mean wind direction. This is the highest reported frequency via satellite and these waves should be quite well adjusted to the wind direction for the slowly turning winds encountered.

7 CONCLUSION

For this experiment, a wavestaff and a bi-axial current meter are used as "reference" to which are compared the NDBC/SWADE 3 meter discus directional data. However, it should be emphasized that both of these systems have equal directional resolution, in principle. In fact the current meter precision diminishes rapidly with depth of immersion and the general results from such triplets may be greatly influenced by the presence of a strong mean current (Forristall *et al.* 1978). It appears, however, that for this particular experiment, the directional parameters produced by the wavestaff and current meter triplets are reasonable up to frequencies of about 0.35 Hz.

Over the years, non directional wave followers have been known for their reliability and their capacity to measure surface displacement adequately. The NDBC/SWADE buoy is no exception, it compares favorably with the wavestaff of the Bullwinkle platform. The variances of both signals were similar, as were the spectral energy distribution and probability distributions.

Directional properties are inherently more variable and thus more difficult to compare. However we have shown that buoy and platform yield similar results for mean direction and directional width particularly if comparison is restricted to sea states in excess of 1 m. Both systems are clearly operating at the edge of their range in smaller waves. Higher order statistics (skewness and kurtosis) of the directional properties are poorly correlated, but it is not clear that either system has the necessary directional resolving power to describe these adequately.

In general these comparisons indicate that the NDBC/SWADE 3 meter discus directional buoy performs as well as the best of the pitch-roll buoy systems assesed by Allender *et al.* (1989) in a similar buoy/platform comparison.

Finally it should be emphasized that the detailed comparison and the general comparison are based on only 68 and 195 records respectively, none of which includes particularly large storms. However, since the agreement between directional parameters improves with higher waves, it is believed that the conclusions of this experiment will hold for more energetic sea states.

8 ACKNOWLEDGEMENTS

The authors acknowledge the excellent collaboration of the National Data Buoy Center personnel for the preparation, calibration and mooring of the buoy, and Shell Development Company for having provided the Bullwinkle platform data. Technical support rendered by Roland Desrosiers and Joe Gabriele, of the National Water Research Institute, is also gratefully acknowledged. This work is part of the preparation for the Surface Wave Dynamics Experiment (SWADE), supported by the Office of Naval Research under contract No. N00014-88-J-1028. F.A. was supported on scholarship by the Natural Sciences and Engineering Research Council of Canada.

9 REFERENCES

Allender, J., Audunson, T., Barstow, S.F., Bjerken, S., Krogstad, H., Steinbakke, P., Vartdal, L., Borgman, L. and Graham, C. 1989. The Wadic Project: A comprehensive field evaluation of directional wave instrumentation. *Ocean Eng.*, **16** (5/6): 505-536.

Borgman, L.E. 1982. Techniques for computer simulation of oceans waves. *Topics in Ocean Physics*, A.R. Malanotte Rizzoli, Ed., Noord-Hollnad, 347-417.

Cartwright, D.E. and Longuet-Higgins, M.S. 1956. The statistical distribution of the maxima of a random fuction. *Proc. R. Soc. Lond.*, **A237**: 212-232.

Digre, K.A., Brasted, L.K. and Marshall, P.W. 1989. The design of the Bullwinkle Platform. *Offshore Tech. Conf.*, OTC 6050, 63-80.

Donelan, M.A. and Pierson., W.J. 1983. The sampling variability of estimates of spectra of wind-generated waves. J. Geophys. Res., **88** (C7): 4381-4392.

Donelan, M.A. Hamilton, J. and Hui, W.H. 1985. Directional spectra of wind-generated waves. *Phil. Trans. R. Soc. Lond.*, **A315**: 509-562.

Forristall, G.Z. 1981. Measurements of the saturated range in ocean wave spectra. *J. Geophys. Res.*, **86** (C9): 8075-8084.

Forristall, G.Z., Ward, E.G. Cardone, V.J. and Borgman, L.E. 1978. The directional spectra and kinematics of surface gravity waves in tropical storm Delia. *J. Phys. Oceanogr.*, **8** (5): 888-909.

Goda, Y. 1985. *Random Seas and Design of Maritime Structures*. University of Tokyo Press, Tokyo, 323 p.

Harris, F.J. 1978. On the use of windows for harmonic analysis with the discrete Fourier transform. *Proc. of the IEEE*, **66** (1): 51-83.

James, I.D. 1986. A note on the theoretical comparison of wave staffs and wave rider buoys in steep gravity waves. *Ocean Engng.*, **13** (2): 209-214.

Kahma, K.K. 1981. A study of the growth of the wave spectrum with fetch. *J. Phys. Oceanogr.*, **11**: 1503-1515.

Kim, W.D. 1966. On a free-floating ship in waves. *J. Ship Res.*, **10**: 181-191.

Kuik, A.J., van Vledder, G.Ph. and Holthuijsen, L.H. 1988. A method for the routine analysis of pitch-and-roll buoy wave data. *J. Phys. Oceanogr.*, **18** (7): 1020-1034.

Long, R.B. 1980. The statistical evaluation of directional spectrum estimates derived from pitch/roll buoy data. *J. Phys. Oceanogr.*, **10**: 944-952.

Longuet-Higgins, M.S. 1952. On the statistical distributions of the heights of sea waves. *J. Mar. Res.*, **IX** (3): 245-266.

Longuet-Higgins, M.S. 1983. On the joint distribution of wave periods and amplitudes in a random wave field. *Proc. R. Soc. Lond.*, **A389** : 241-258.

Longuet-Higgins, M.S. 1986. Eularian and Lagrangian aspects of surface waves. *J. Fluid Mech.*, **173**: 683-707.

Longuet-Higgins, M.S., Cartwright, D.E. and Smith, N.D. 1963. Observations of the directional spectrum of sea waves using the motions of a floating buoy. *Ocean Wave Spectra.* Prentice-Hall, Englewood Cliff, New Jersey, 111-136.

Ochi, M.K. 1982. Stochastic analysis and probabilistic prediction of random seas. *Advances in Hydroscience*, Academic Press, **13**: 217-375.

Pierson, W.J. 1983. The measurement of the synoptic scale wind over the ocean. *J. Geophys. Res.*, **88** (C3): 1683-1708.

Steele, K.E., Lau, J.C.K. and Hsu, Y.H.L., 1985: Theory and application of calibration techniques for an NDBC directional wave measurements buoy. *IEEE J. Oceanic Eng.*, OE-10(4), 382-396.

Steele, K.E., Wang, W.C., Teng, C.C. and Lang, N.C., 1990: *Directional-wave measurements with NDBC 3-meter discus buoys.* National Data Buoy Center, Report 1804-01.05, U.S. Department of Commerce, Mississippi, 35 p.

Stewart, R.H. 1977. A discus-hulled wave measuring buoy. *Ocean Engng.*, **4**: 101-107.

Swanson, R.C. and Baxter, G.D. 1989. The Bullwinkle platform instrumentation system. *Offshore Tech. Conf.*, OTC 6052, 93-100.

The MathWorks. 1988. *Signal Processing Toolbox User's Guide.* South Natick, Massachusetts, 167 p.

Welch, P.D. 1967. The use of fast Fourier transform for the estimation of power spectra: a method based on time averaging over short, modified periodograms. *IEEE Trans. Audio and Electroacoust.*, **AU-15**: 70-73.

Weller, R.A., Donelan, M.A. Briscoe, M.G. and Huang, N.E. 1991. Riding the crest: a tale of two experiments. *Bulletin American Meteorological Society*, **72** (2): 163-183.

10 FIGURE CAPTIONS

Figure 1 — Surface displacement spectra as a function of frequency: (—) is the buoy spectrum, (- -) is the platform spectrum, and (— -) represents a slope of ω^{-4}; (a) is characterized by H_s = 1.1 m and T_p = 7.5 s; and (b) is H_s = 0.9 m and T_p = 6.5 s.

Figure 2 — NDBC/SWADE 3 meter discus directional buoy mean phase shift Φ_h (a) and mean wavenumber ratio R_h (b) from "on board" analysis. Vertical lines indicate the standard deviations over 195 20 minute records.

Figure 3 — Scatter plots of buoy and platform significant wave height, peak period, mean direction at the peak and directional width at the peak.

Figure 4 — Same as 3, but only for records of platform significant wave height greater than 1 meter.

Figure 5 — Environmental conditions for the part of the experiment when both systems were fully operational.

Figure 6 — Scatter plots of buoy and platform surface displacement root-mean-square, skewness and kurtosis values.

Figure 7 — Scatter plots of buoy and platform significant wave height, mean wave period, peak wave period and spectral width parameter.

Figure 8 — Scatter plots of buoy and platform mean level upcrossing mean wave height and period, and mean 1/3 maximum wave height and corresponding periods.

Figure 9 — Various distributions of the buoy surface displacement signal (H_s = 1.1 m, T_p = 7.5 s and ν = 0.36). (a), wave height probability density, where * is measured and (- -) is theoretical (Rayleigh). (b), wave period probability density, where * is measured and (- -) is theoretical (Longuet-Higgins (1983)). (c), surface displacement probability density, where * is measured and (- -) is theoretical (Gaussian). (d), wave height and period joint frequency distribution, where the curves have respective probability of 0.03, 0.1, 0.5 and 1.0. (e), occurence probability of length of run of high waves, where * is above $H_{1/3}$ and + is above $H_{1/10}$.

Figure 10 — Same as 9, except platform measurements are used and ν = 0.40.

Figure 11 — Same as 9, except a different buoy surface displacement signal is used (H_s = 0.9 m, T_p = 6.5 s and ν = 0.36).

Figure 12 — Same as 11, except platform measurements are used and ν = 0.39.

Figure 13 — Scatter plots of buoy and platform mean direction, and directional width, skewness and kurtosis parameters, for all 68 records.

Figure 14 — Scatter plots of buoy and platform mean direction, and directional width, skewness and kurtosis parameters, for records of buoy significant wave height greater than 1 meter.

Figure 15 — Directional parameters as a function of frequency: (—) is the mean direction, deg; (- -) is the directional width, deg; (···) is the power spectrum normalized so that the peak value is 360; (a) is the buoy, and (b) is the platform. The sea is characterized by H_s = 1.1 m and T_p = 7.5 s.

Figure 16 — Same as 13, except the sea is characterized by $H_s = 0.9$ m and $T_p = 6.5$ s.

Figure 17 — Comparison of buoy measured mean wave direction with the wind direction, for the highest frequencies reported via satellite.

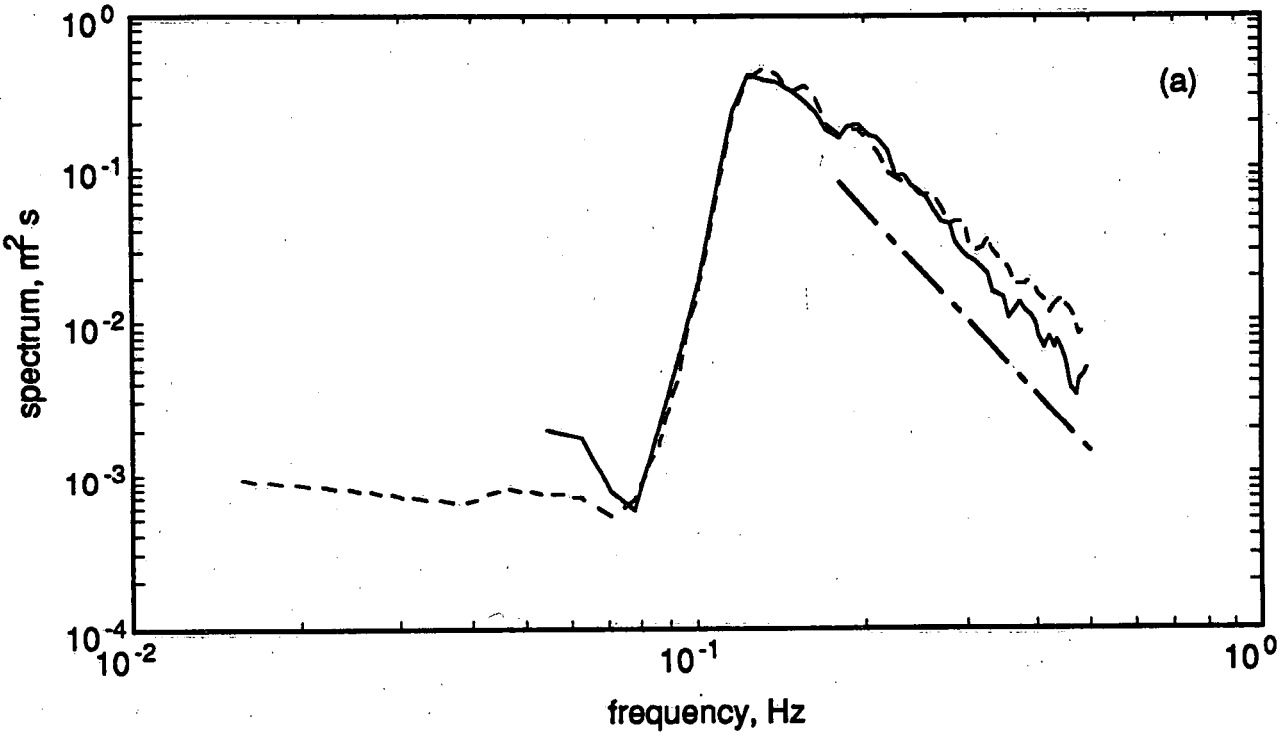
(a)
spectrum, m² s
frequency, Hz
10⁰
10⁻¹
10⁻²
10⁻³
10⁻⁴
10⁻²
10⁻¹
10⁰

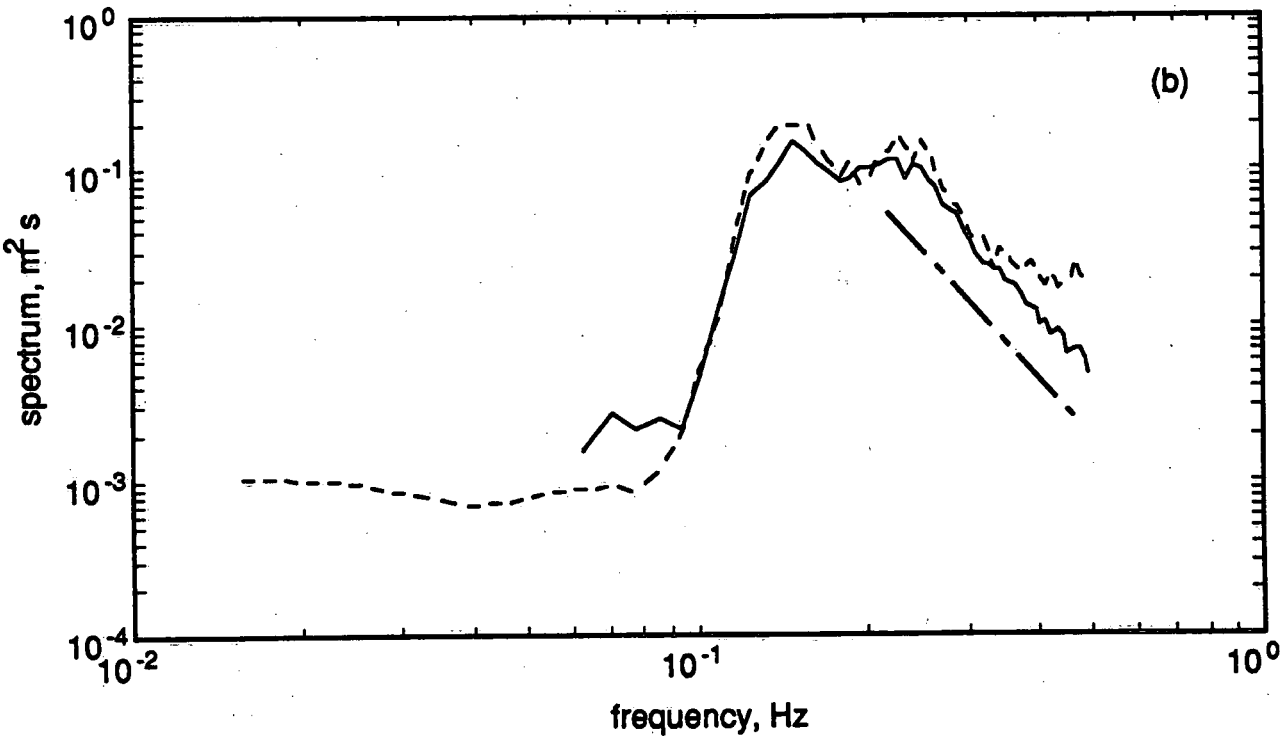
(b)
spectrum, m² s
frequency, Hz
10⁰
10⁻¹
10⁻²
10⁻³
10⁻⁴
10⁻²
10⁻¹
10⁰

Figure 1

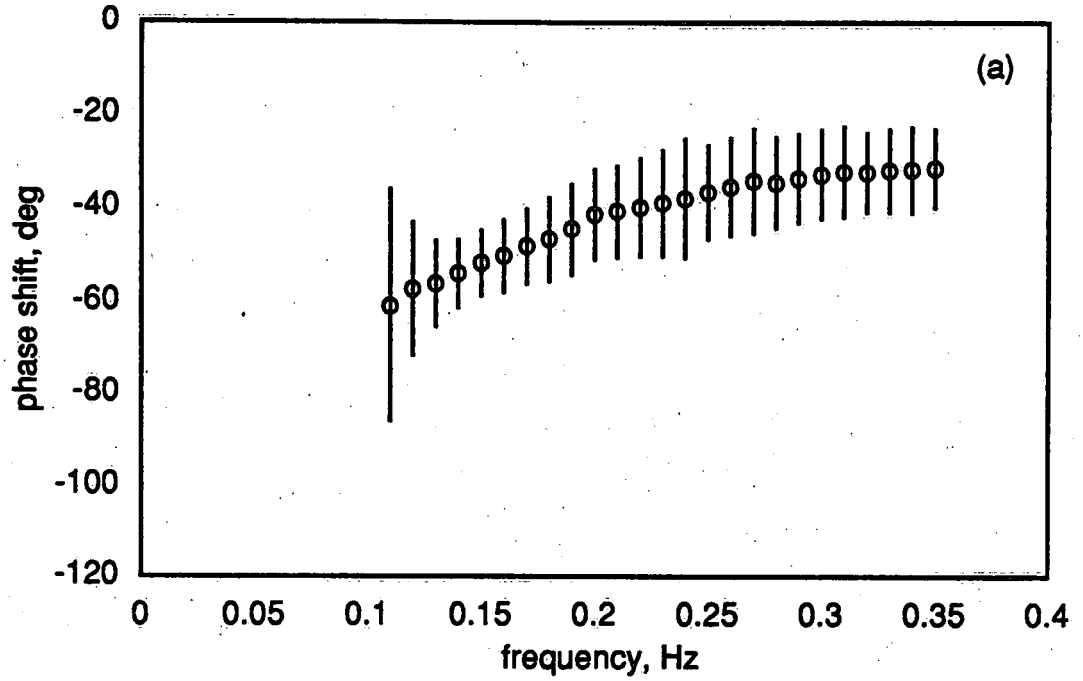
(a)
phase shift, deg
0
-20
-40
-60
-80
-100
-120
0
0.05
0.1
0.15
0.2
0.25
0.3
0.35
0.4
frequency, Hz

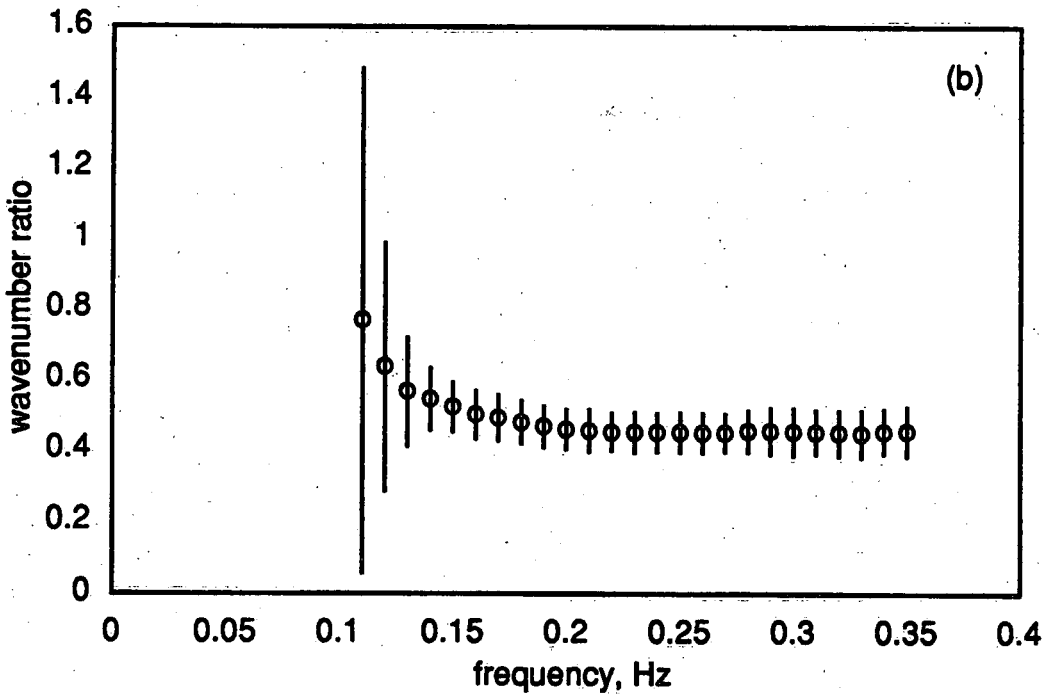
(b)
wavenumber ratio
1.6
1.4
1.2
1
0.8
0.6
0.4
0.2
0
0
0.05
0.1
0.15
0.2
0.25
0.3
0.35
0.4
frequency, Hz

Figure 2

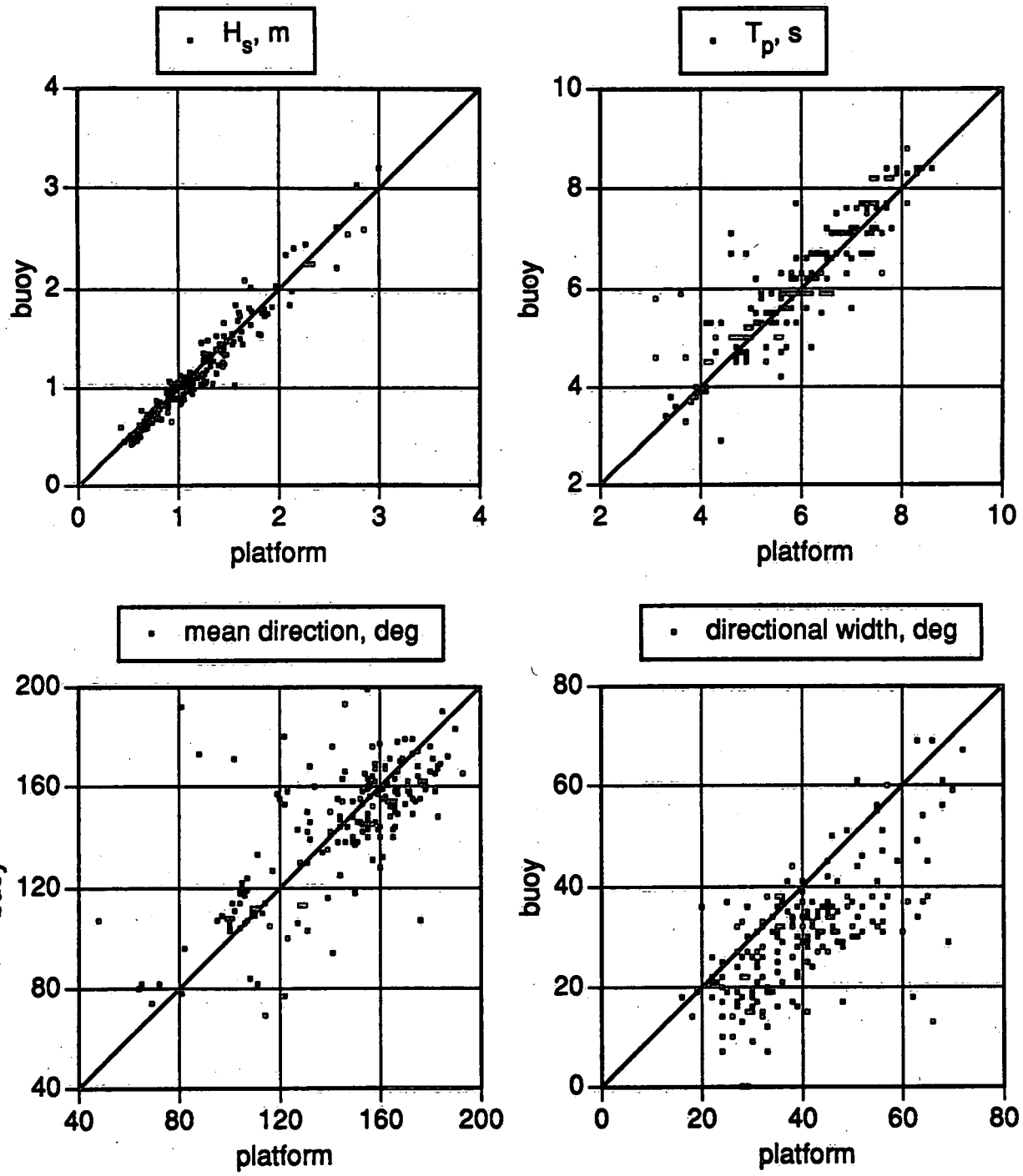
H_s, m
buoy
platform
0
1
2
3
4
T_p, s
buoy
platform
2
4
6
8
10
mean direction, deg
buoy
platform
40
80
120
160
200
directional width, deg
buoy
platform
0
20
40
60
80

Figure 3

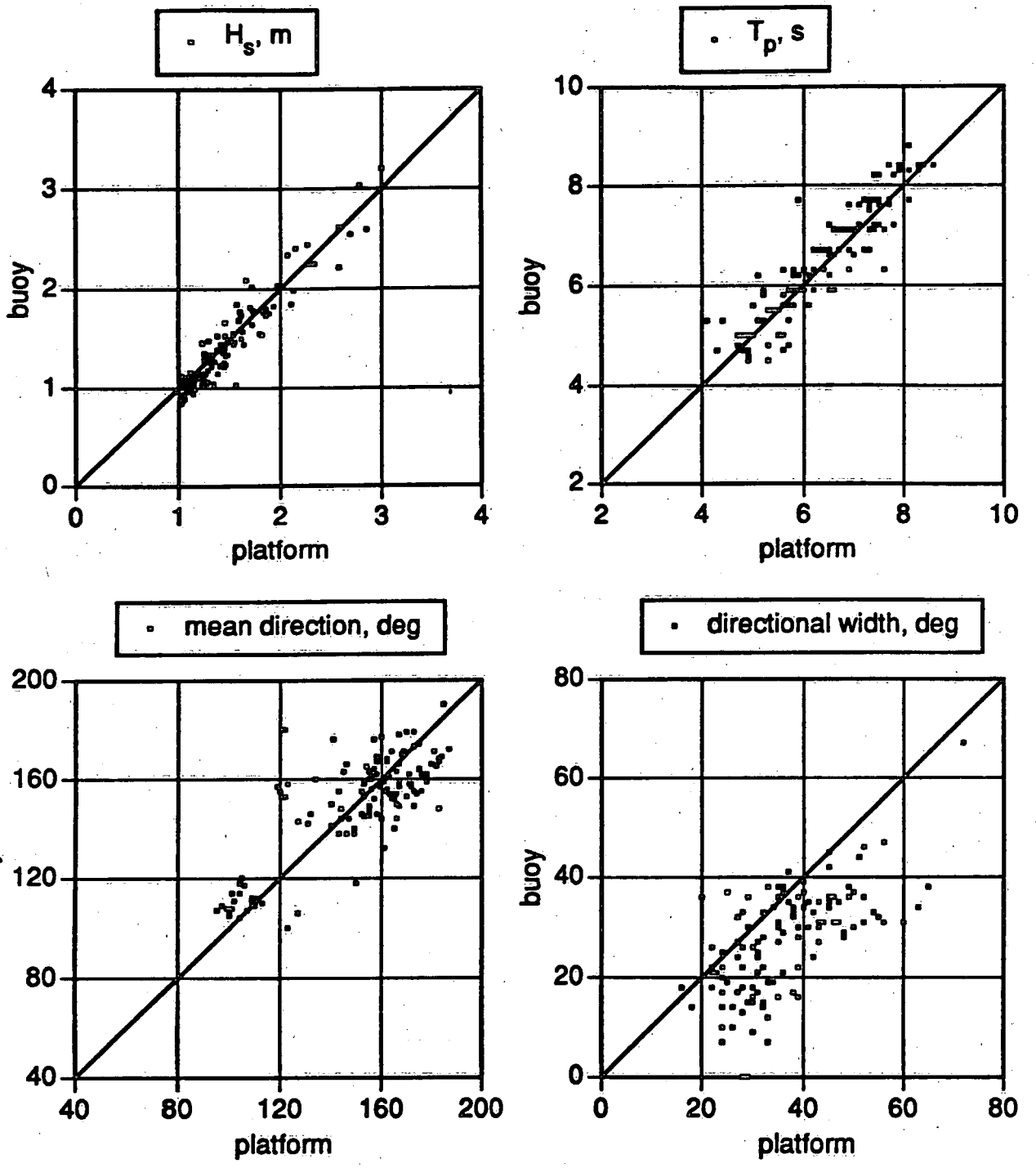
H_s, m
buoy
platform
0
1
2
3
4
T_p, s
buoy
platform
2
4
6
8
10
mean direction, deg
buoy
platform
40
80
120
160
200
directional width, deg
buoy
platform
0
20
40
60
80

Figure 4

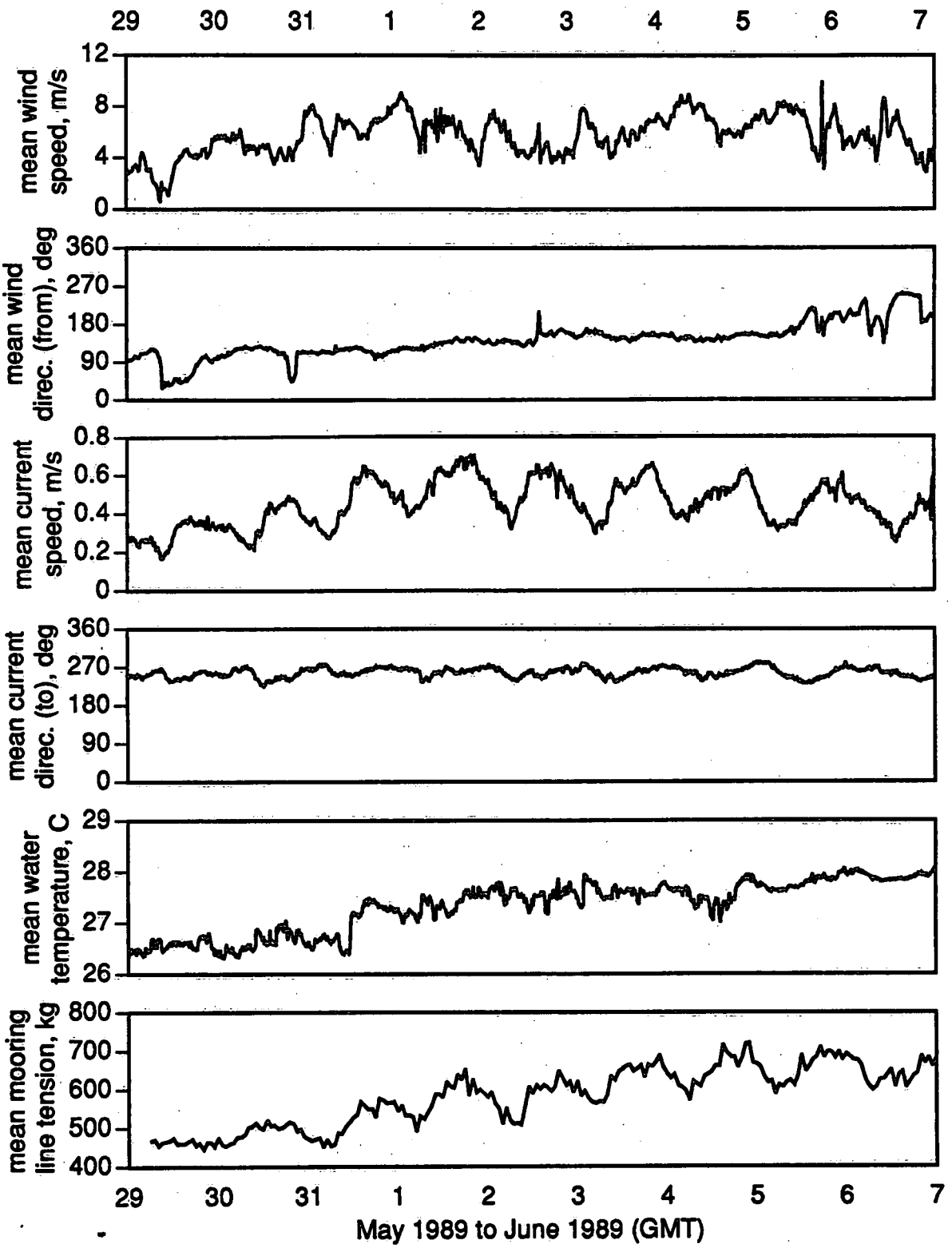
29 30 31 1 2 3 4 5 6 7
mean wind speed, m/s
12
8
4
0
mean wind direc. (from), deg
360
270
180
90
0
mean current speed, m/s
0.8
0.6
0.4
0.2
0
mean current direc. (to), deg
360
270
180
90
0
mean water temperature, C
29
28
27
26
mean mooring line tension, kg
800
700
600
500
400
29 30 31 1 2 3 4 5 6 7
May 1989 to June 1989 (GMT)

Figure 5

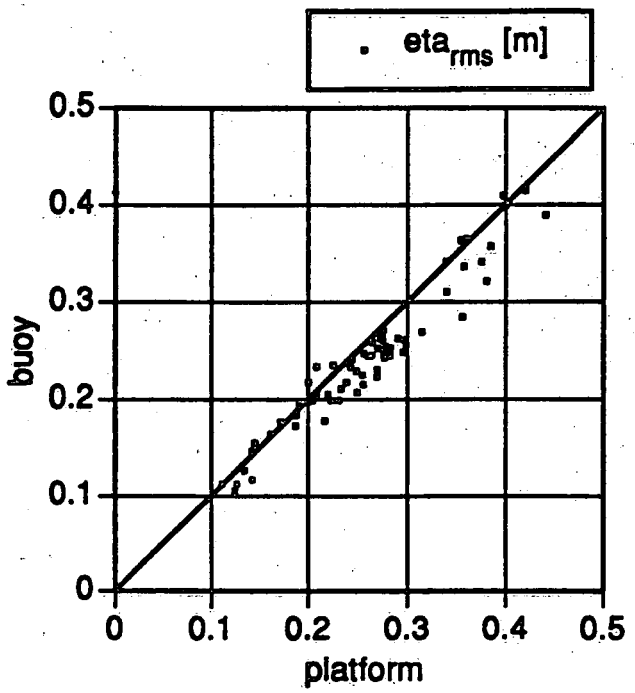
eta$_{rms}$ [m]
0.5
0.4
0.3
0.2
0.1
0
buoy
0
0.1
0.2
0.3
0.4
0.5
platform

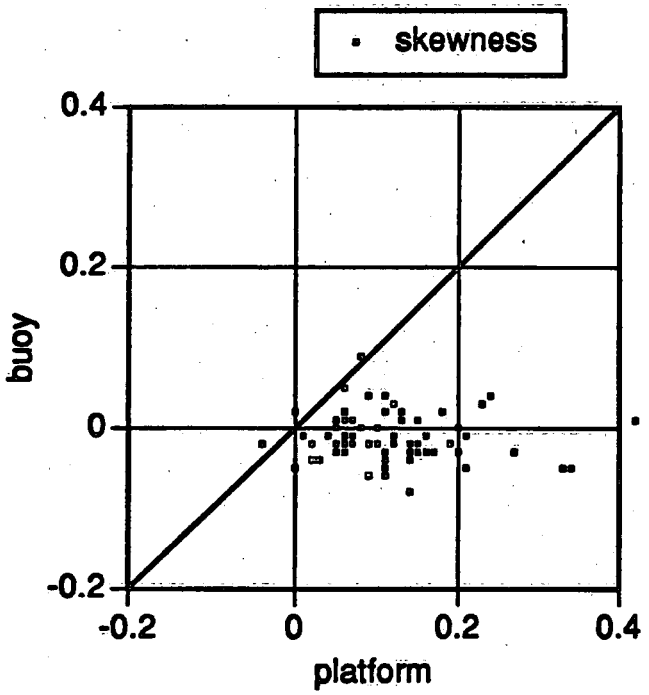
skewness
0.4
0.2
0
-0.2
buoy
-0.2
0
0.2
0.4
platform

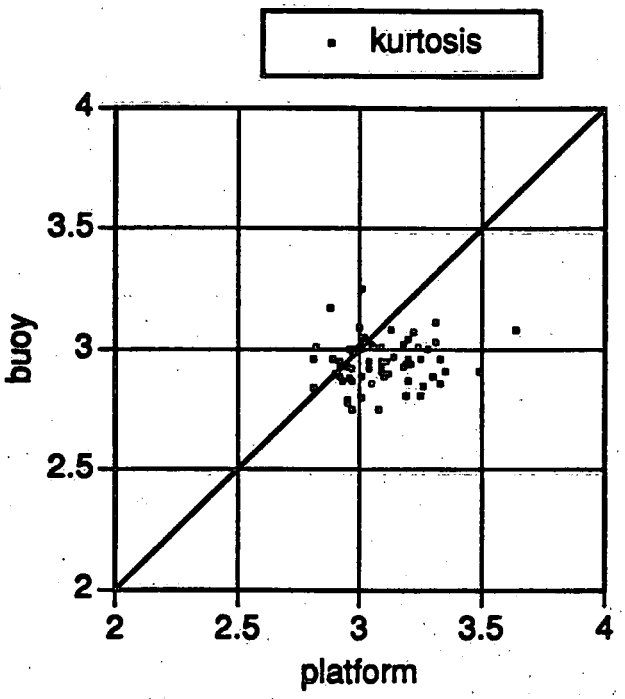
kurtosis
4
3.5
3
2.5
2
buoy
2
2.5
3
3.5
4
platform

Figure 6

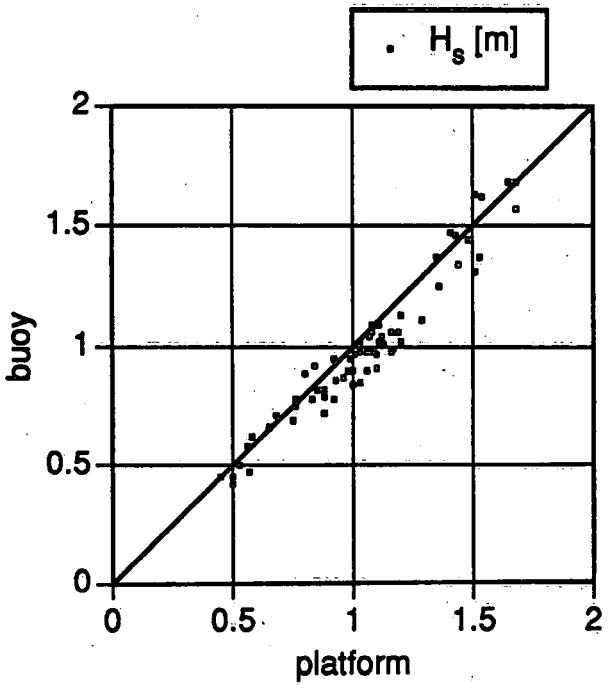
H_s [m]
buoy
platform
0
0.5
1
1.5
2

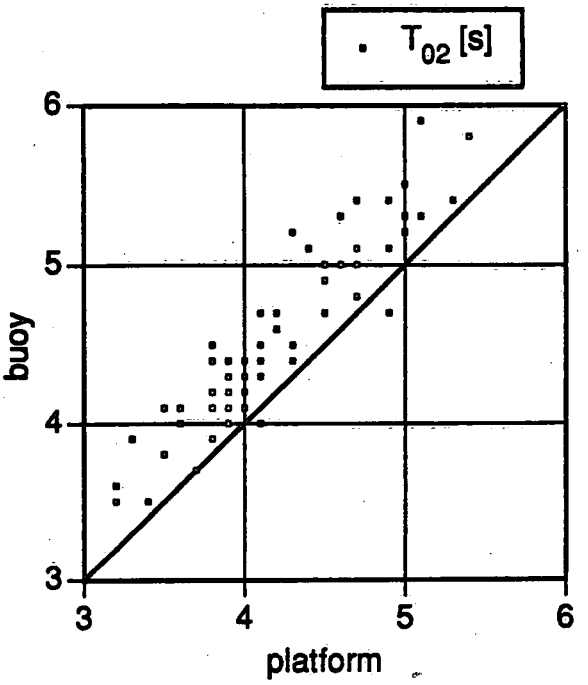
T_{02} [s]
buoy
platform
3
4
5
6

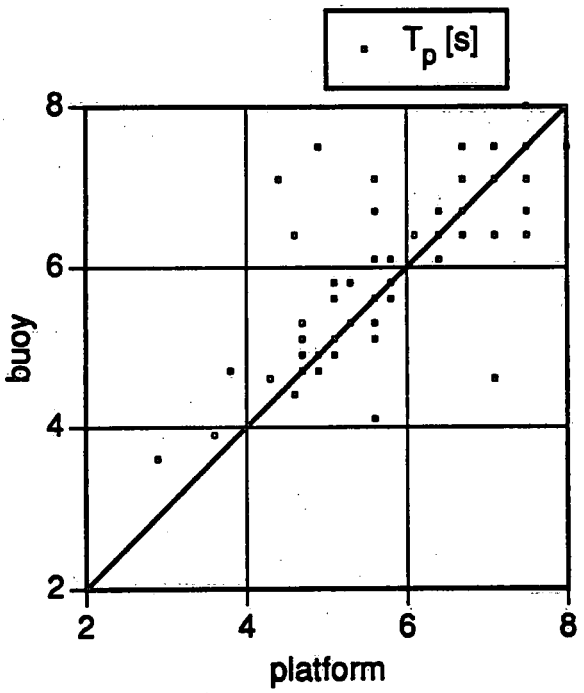
T_p [s]
buoy
platform
2
4
6
8

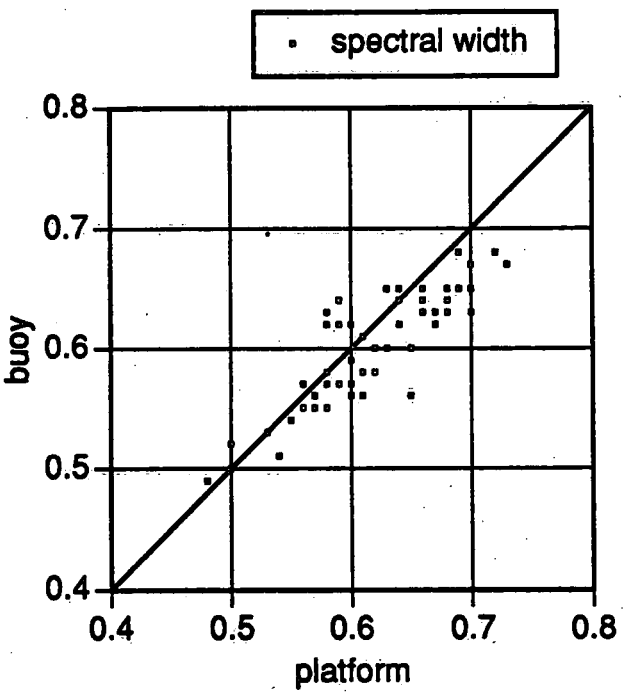
spectral width
buoy
platform
0.4
0.5
0.6
0.7
0.8

Figure 7

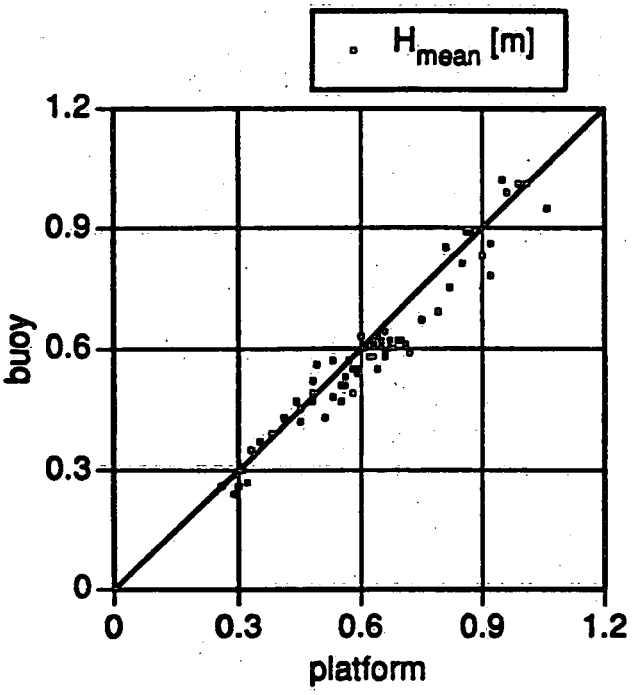
H_{mean} [m]
buoy
platform
0
0.3
0.6
0.9
1.2

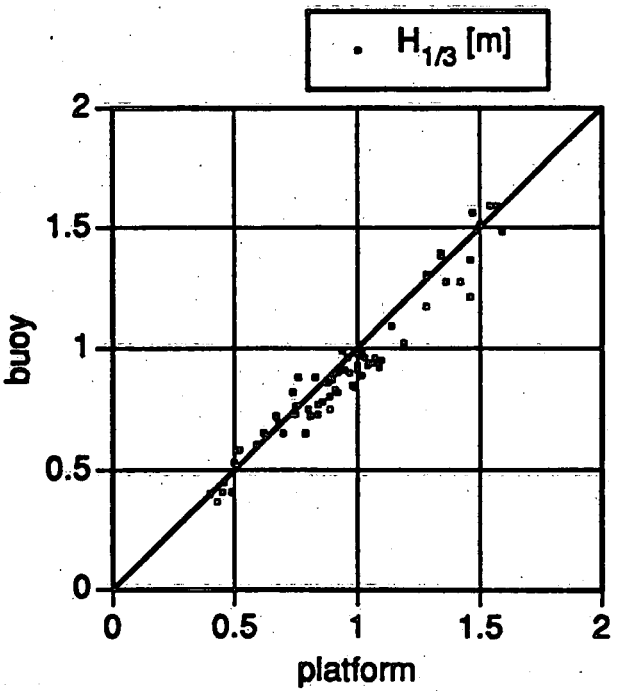
$H_{1/3}$ [m]
buoy
platform
0
0.5
1
1.5
2

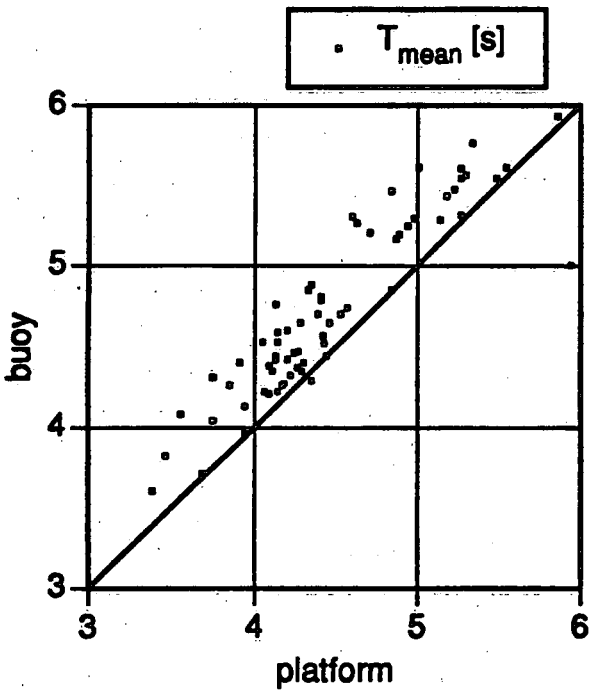
T_{mean} [s]
buoy
platform
3
4
5
6

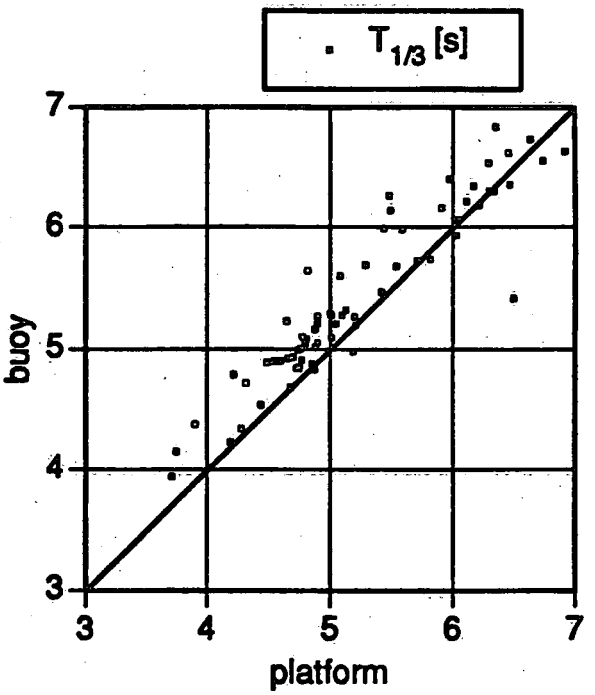
$T_{1/3}$ [s]
buoy
platform
3
4
5
6
7

Figure 5

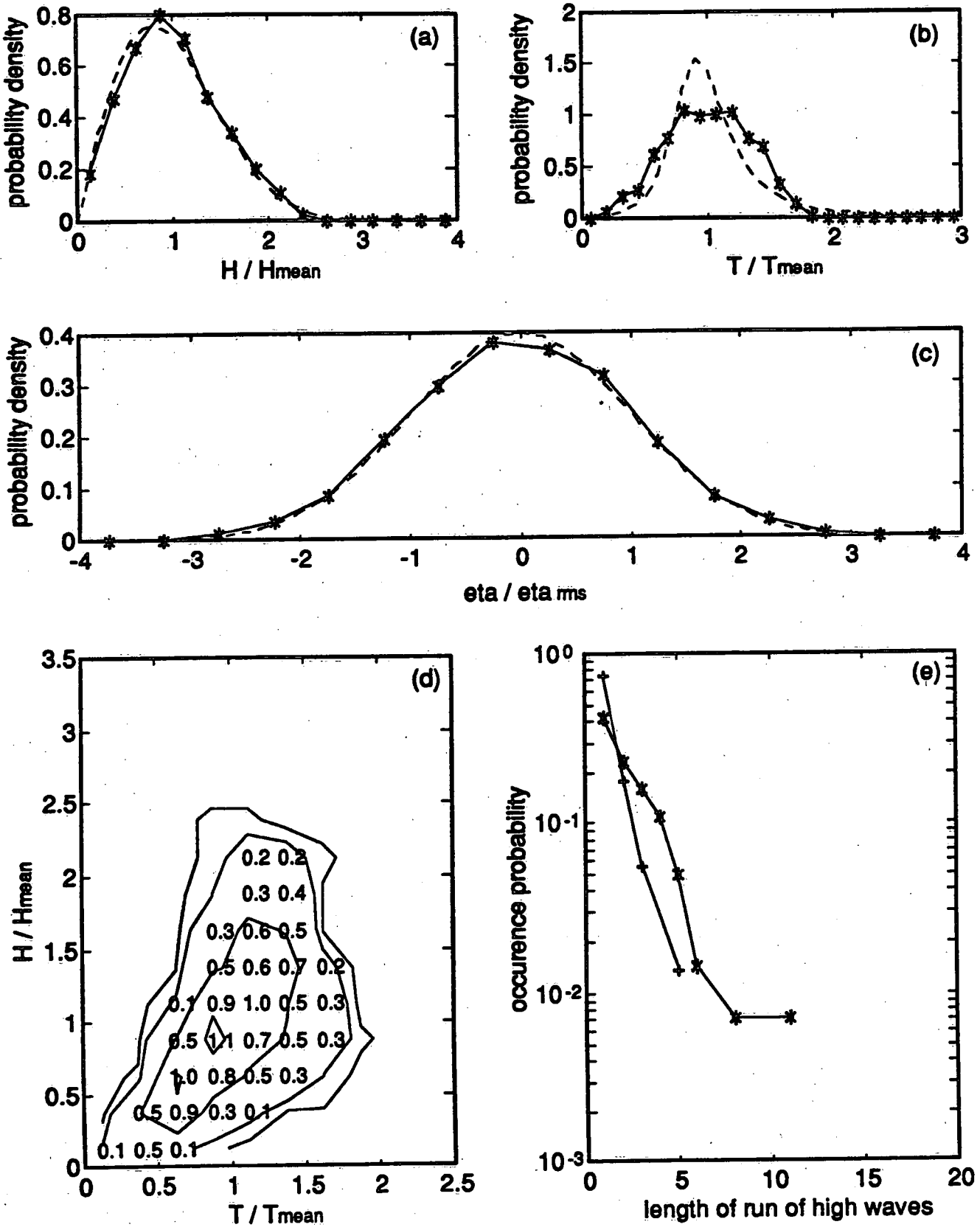
(a)
probability density
H / Hmean
(b)
probability density
T / Tmean
(c)
probability density
eta / eta rms
(d)
H / Hmean
T / Tmean
0.2 0.2
0.3 0.4
0.3 0.6 0.5
0.5 0.6 0.7 0.2
0.1 0.9 1.0 0.5 0.3
0.5 1.1 0.7 0.5 0.3
1.0 0.8 0.5 0.3
0.5 0.9 0.3 0.1
0.1 0.5 0.1
(e)
occurence probability
length of run of high waves

Figure 9

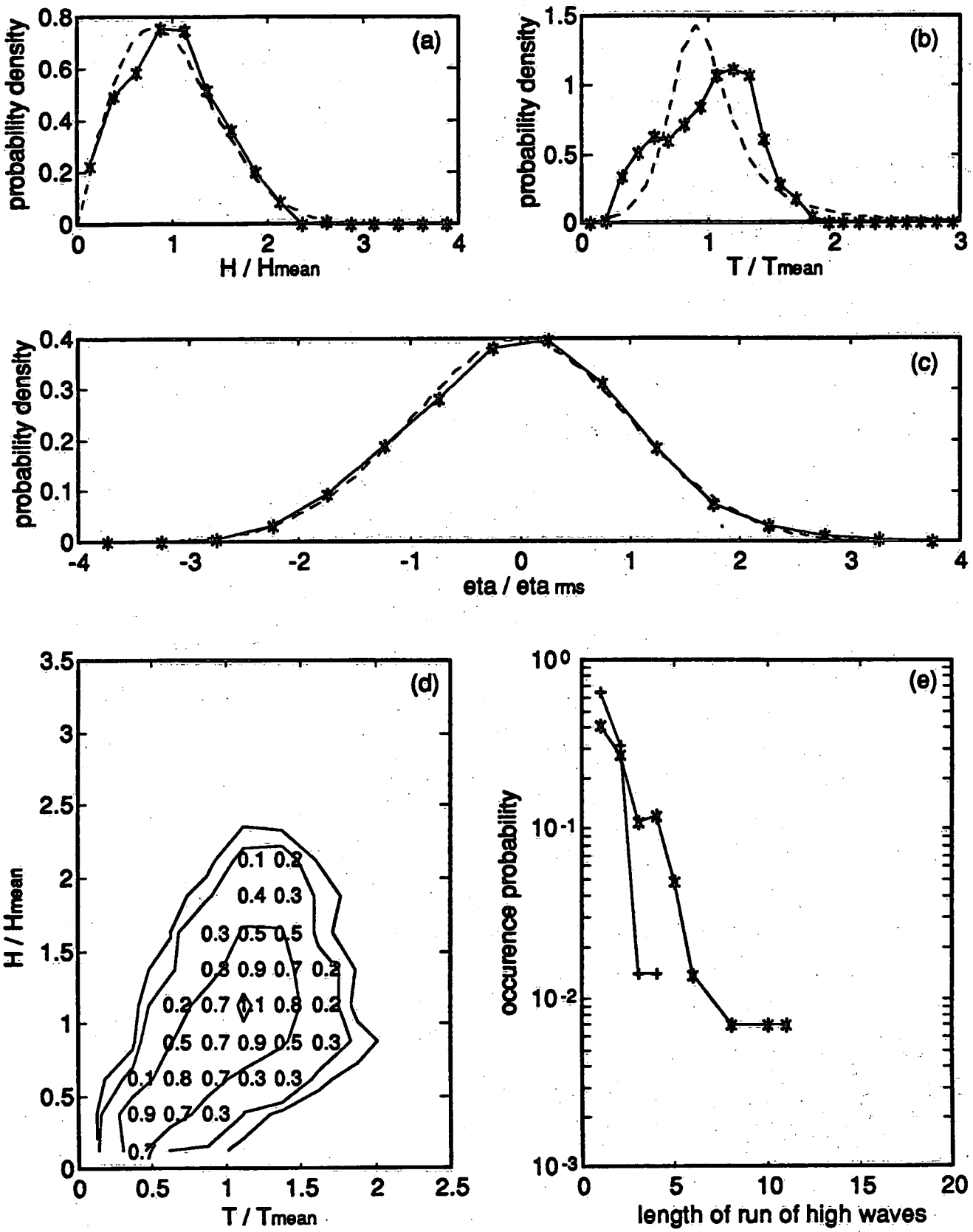
(a)
probability density
H / Hmean
(b)
probability density
T / Tmean
(c)
probability density
eta / eta rms
(d)
H / Hmean
T / Tmean
0.1 0.2
0.4 0.3
0.3 0.5 0.5
0.8 0.9 0.7 0.2
0.2 0.7 0.1 0.8 0.2
0.5 0.7 0.9 0.5 0.3
0.1 0.8 0.7 0.3 0.3
0.9 0.7 0.3
0.7
(e)
occurence probability
length of run of high waves

Figure 15

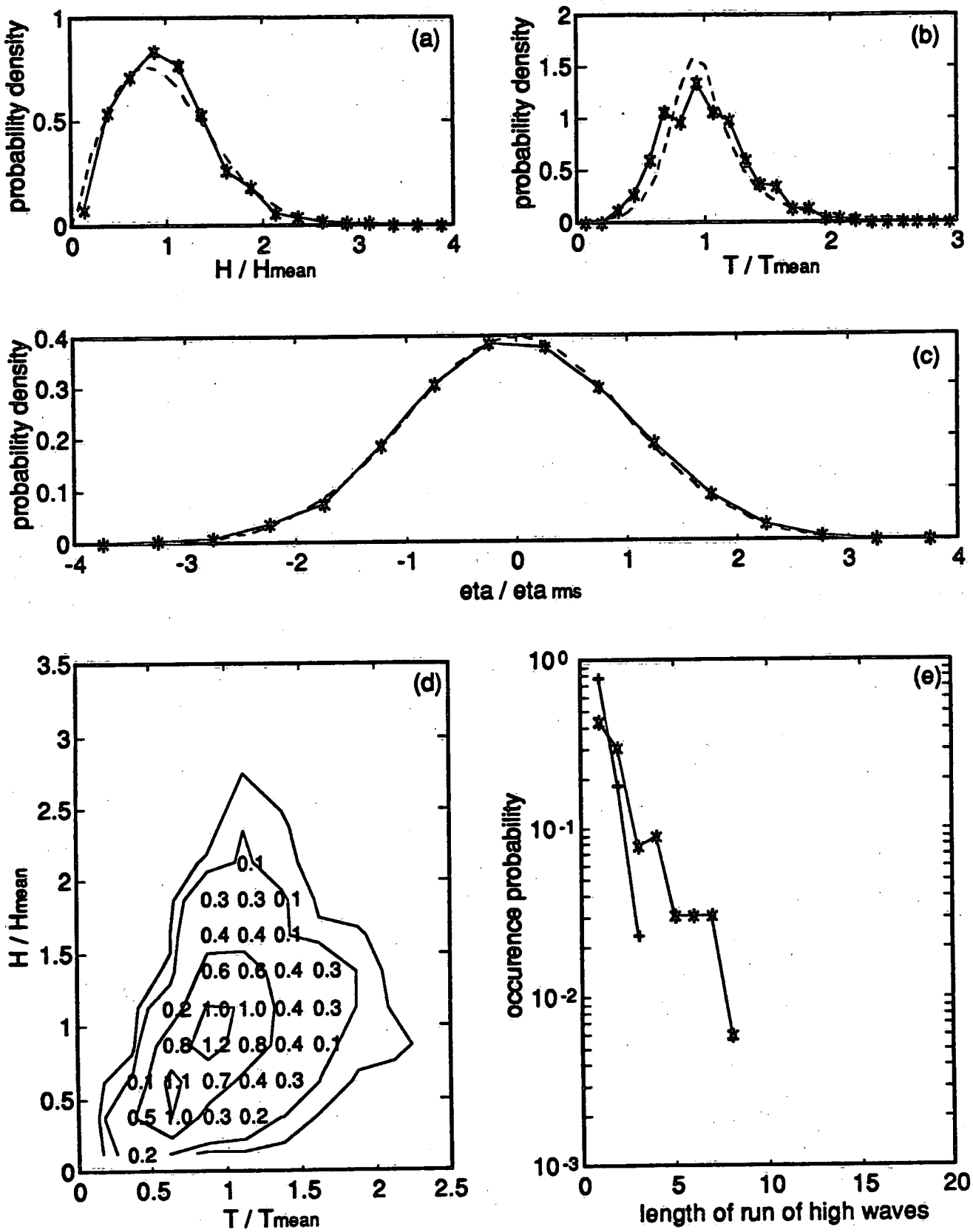
(a)
probability density
H / Hmean
(b)
probability density
T / Tmean
(c)
probability density
eta / eta rms
(d)
H / Hmean
T / Tmean
0.1
0.3 0.3 0.1
0.4 0.4 0.1
0.6 0.6 0.4 0.3
0.2 1.0 1.0 0.4 0.3
0.8 1.2 0.8 0.4 0.1
0.1 0.1 0.7 0.4 0.3
0.5 1.0 0.3 0.2
0.2
(e)
occurence probability
length of run of high waves

Figure 11

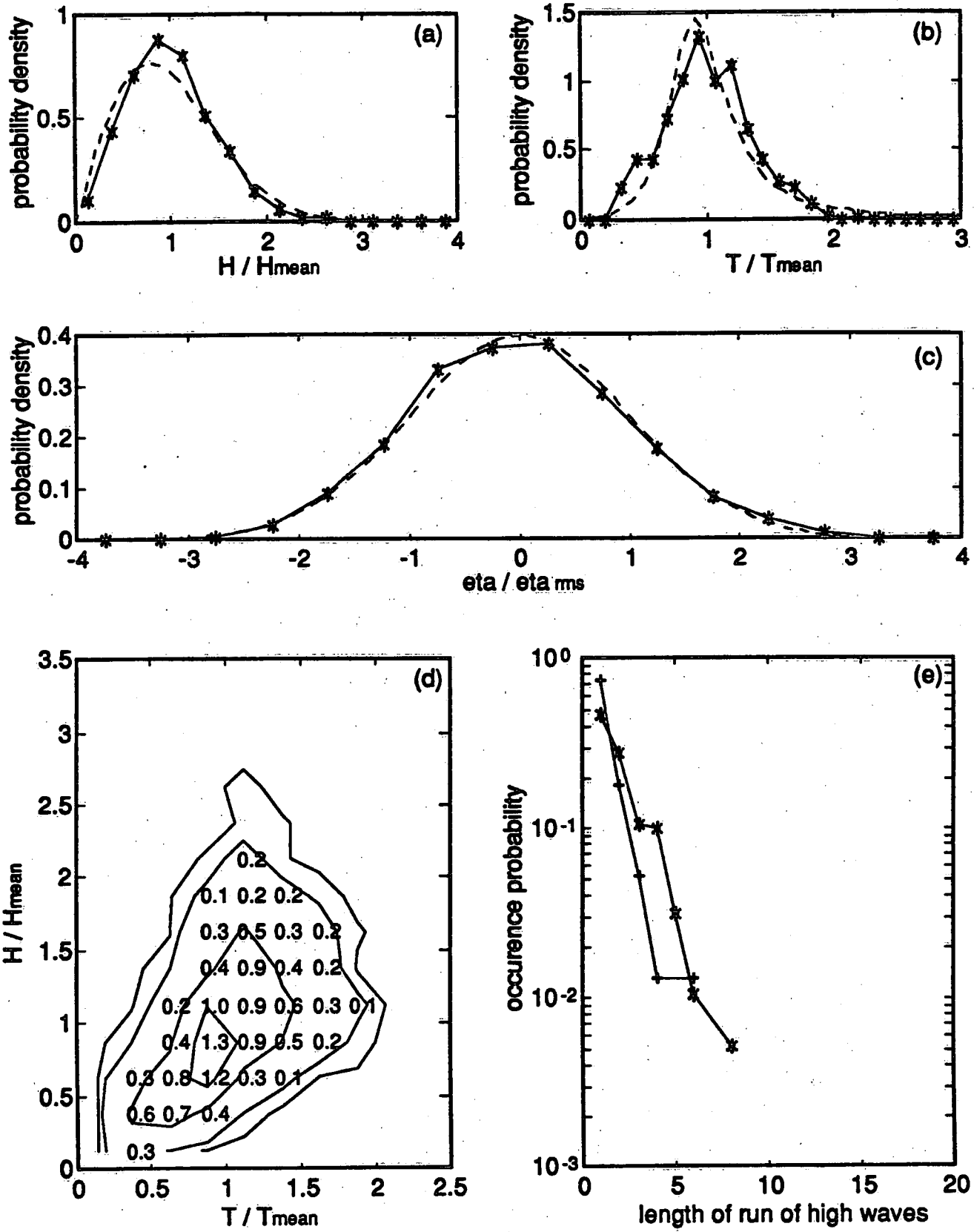
(a)
probability density
H / Hmean
(b)
probability density
T / Tmean
(c)
probability density
eta / eta rms
(d)
H / Hmean
T / Tmean
0.2
0.1 0.2 0.2
0.3 0.5 0.3 0.2
0.4 0.9 0.4 0.2
0.2 1.0 0.9 0.6 0.3 0.1
0.4 1.3 0.9 0.5 0.2
0.3 0.8 1.2 0.3 0.1
0.6 0.7 0.4
0.3
(e)
occurence probability
length of run of high waves

Figure 12

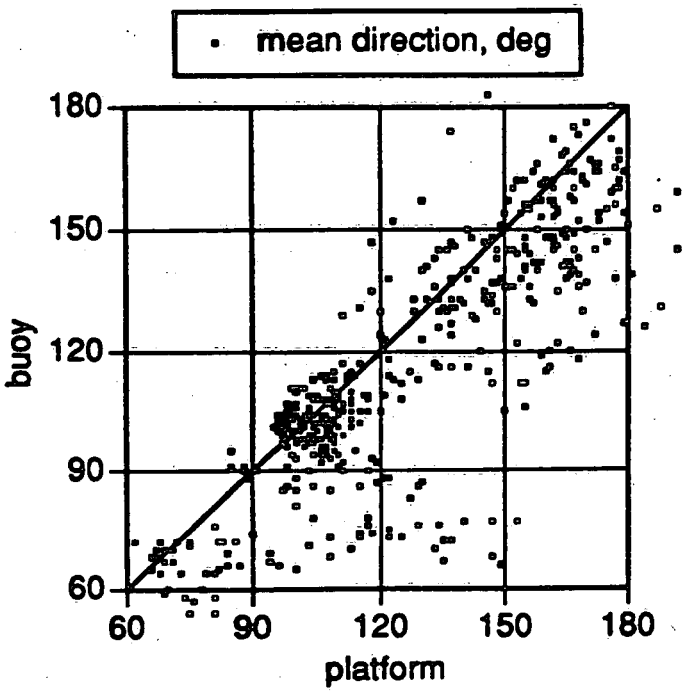
mean direction, deg
180
150
120
90
60
buoy
60
90
120
150
180
platform

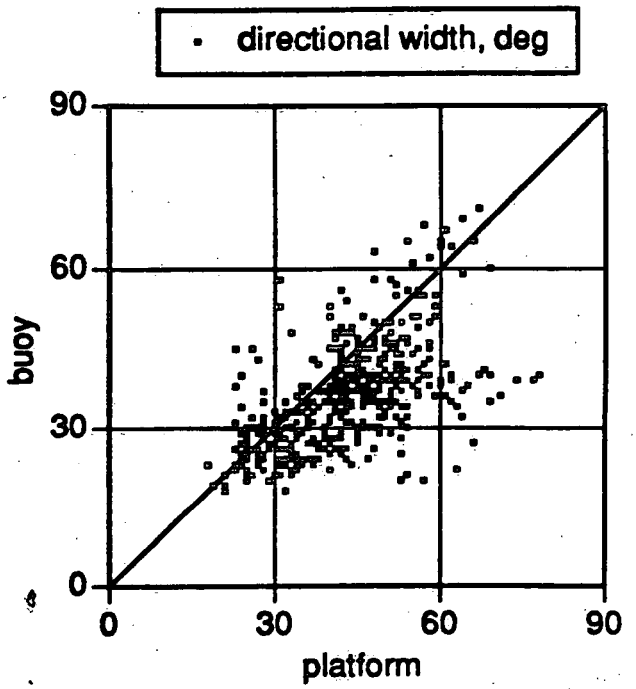
directional width, deg
90
60
30
0
buoy
0
30
60
90
platform

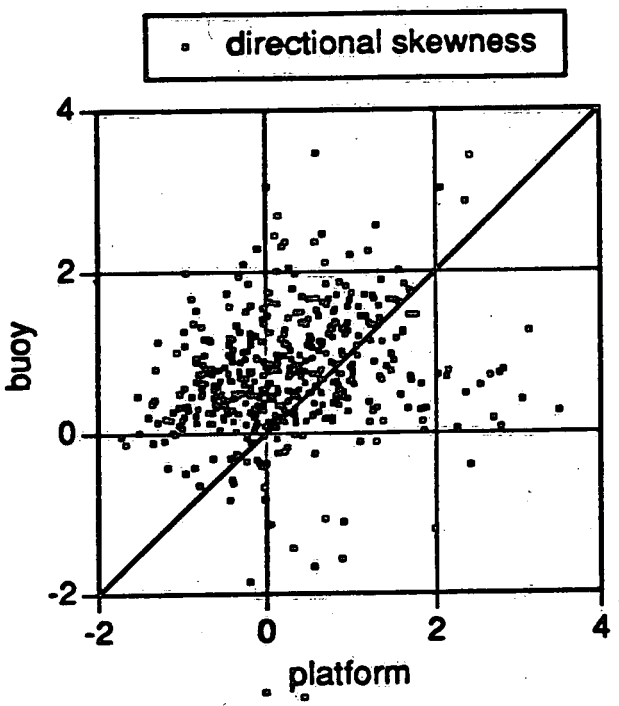
directional skewness
4
2
0
-2
buoy
-2
0
2
4
platform

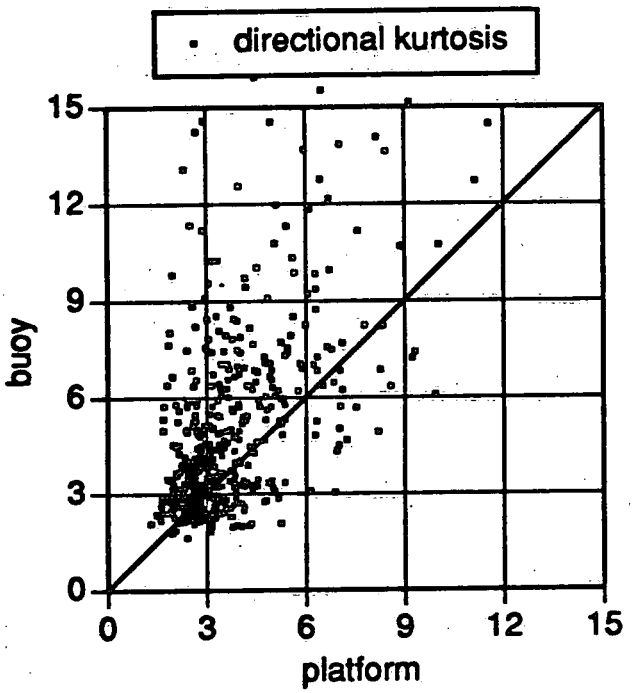
directional kurtosis
15
12
9
6
3
0
buoy
0
3
6
9
12
15
platform

Figure 13

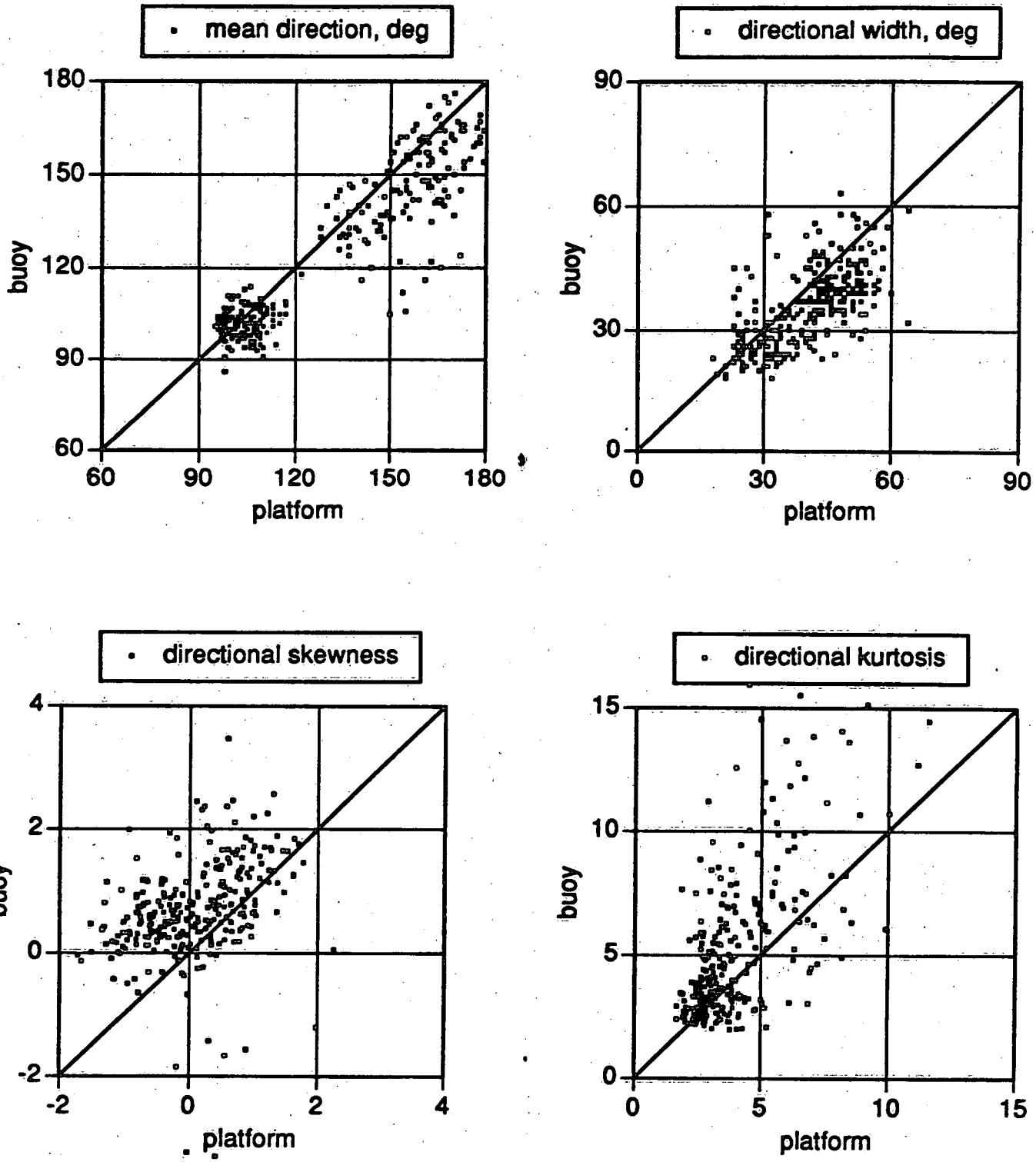
mean direction, deg
180
150
120
90
60
buoy
60
90
120
150
180
platform
directional width, deg
90
60
30
0
buoy
0
30
60
90
platform
directional skewness
4
2
0
-2
buoy
-2
0
2
4
platform
directional kurtosis
15
10
5
0
buoy
0
5
10
15
platform

Figure 14

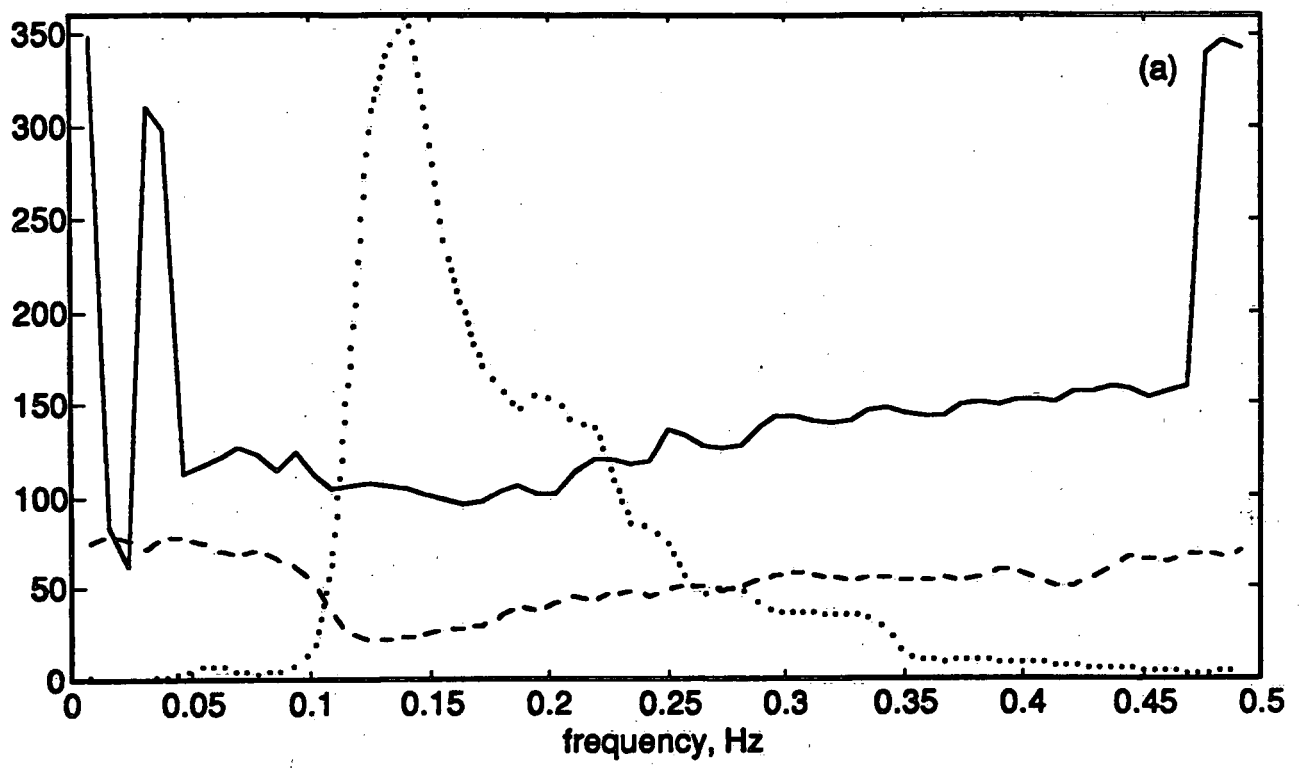
(a)
350
300
250
200
150
100
50
0
0
0.05
0.1
0.15
0.2
0.25
0.3
0.35
0.4
0.45
0.5
frequency, Hz

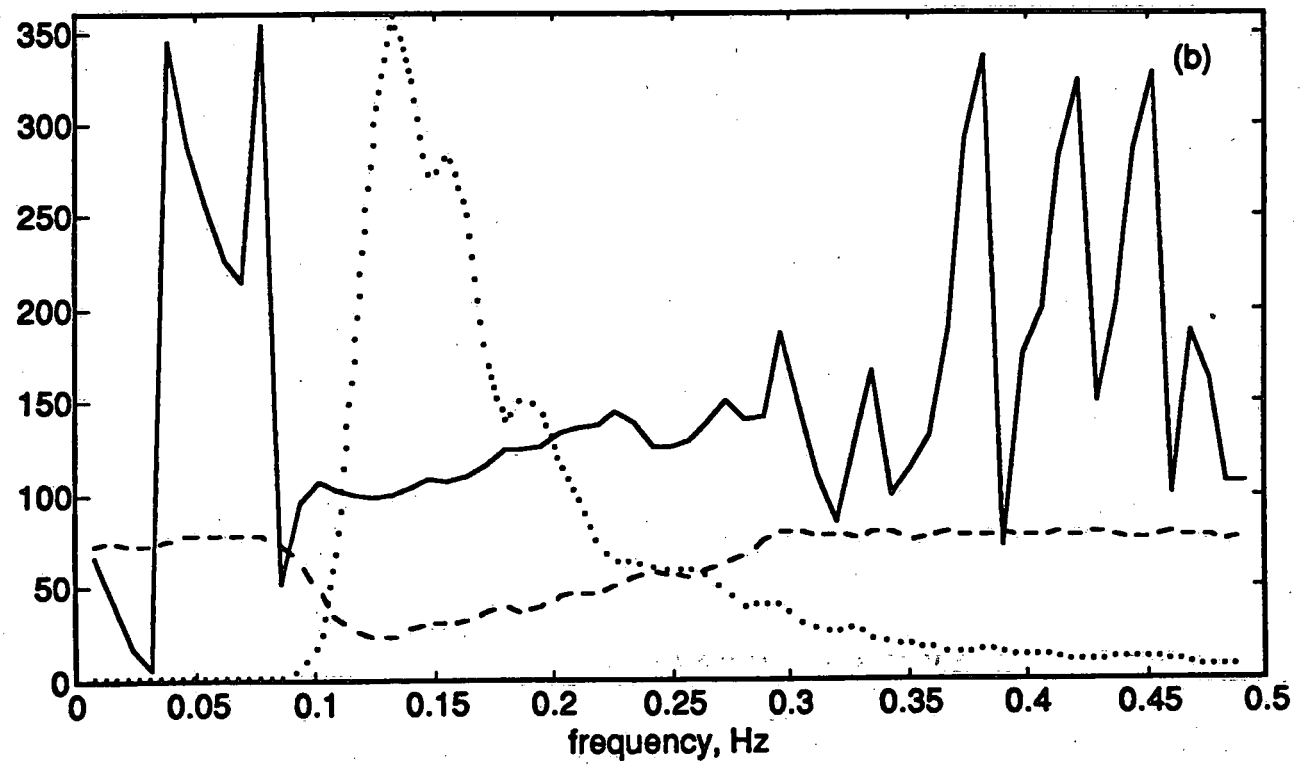
(b)
350
300
250
200
150
100
50
0
0
0.05
0.1
0.15
0.2
0.25
0.3
0.35
0.4
0.45
0.5
frequency, Hz

Figure 15

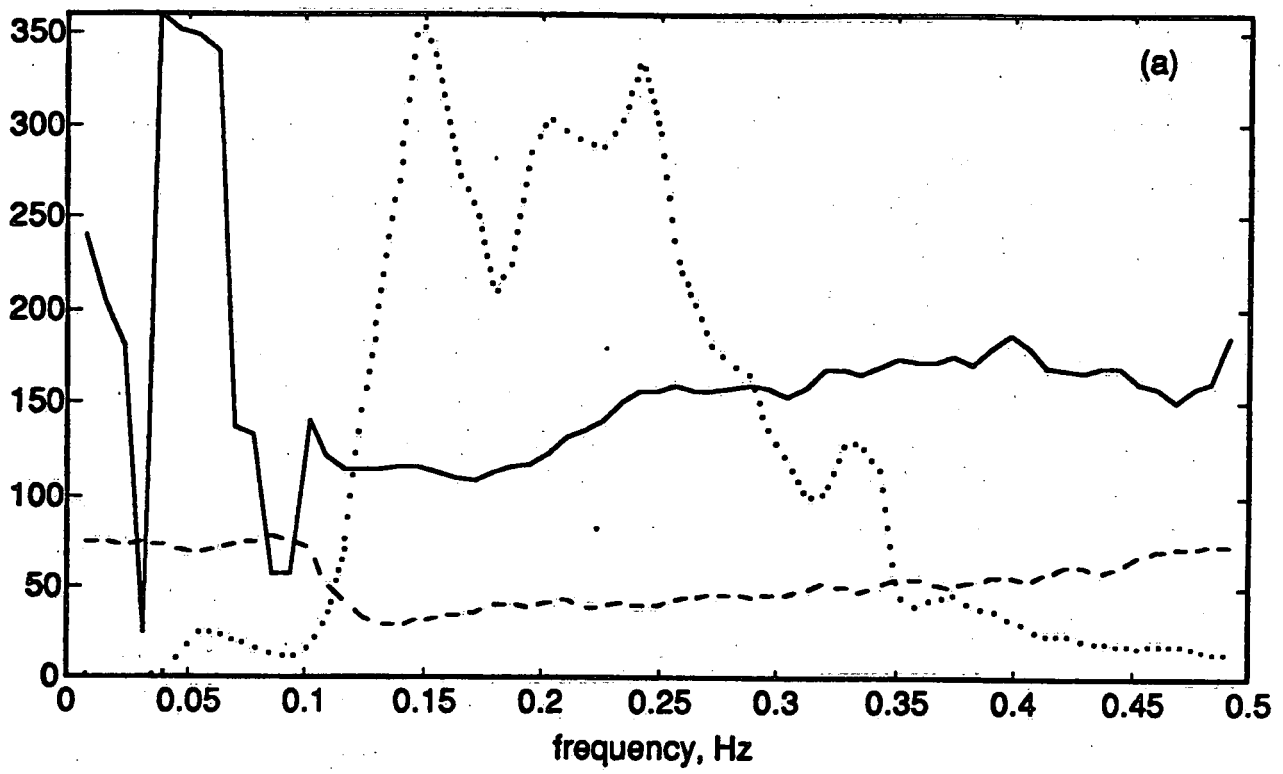
(a)
350
300
250
200
150
100
50
0
0
0.05
0.1
0.15
0.2
0.25
0.3
0.35
0.4
0.45
0.5
frequency, Hz

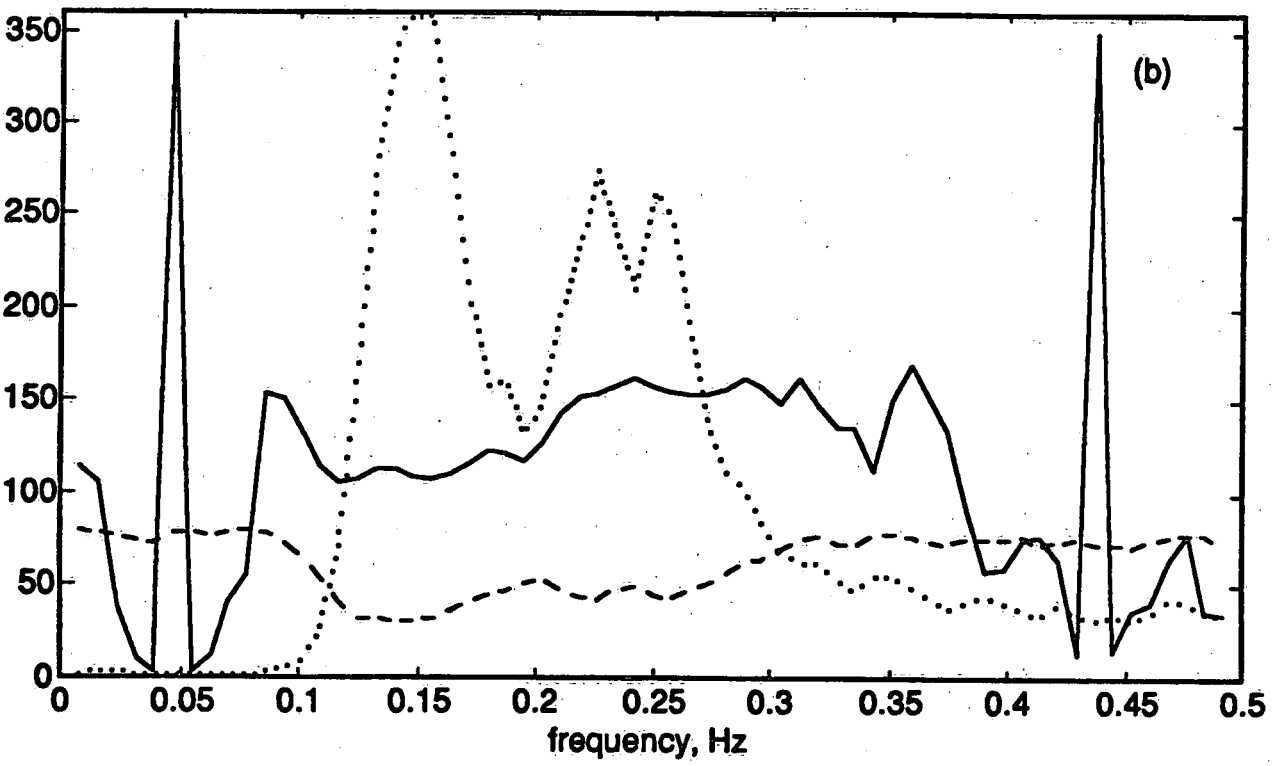
(b)
350
300
250
200
150
100
50
0
0
0.05
0.1
0.15
0.2
0.25
0.3
0.35
0.4
0.45
0.5
frequency, Hz

Figure 16

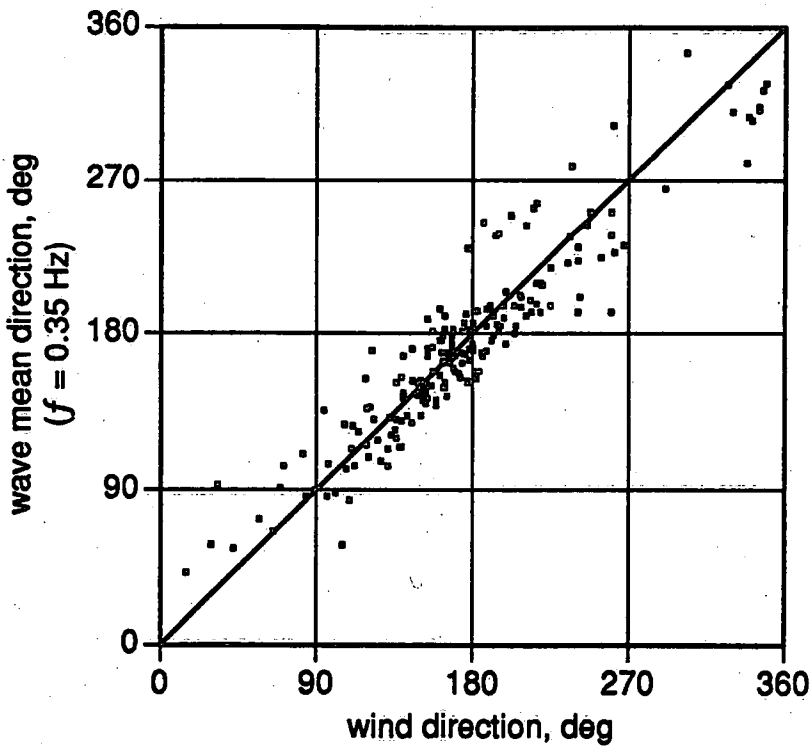
360
270
180
90
0
0
90
180
270
360
wave mean direction, deg
(f = 0.35 Hz)
wind direction, deg

Figure 17

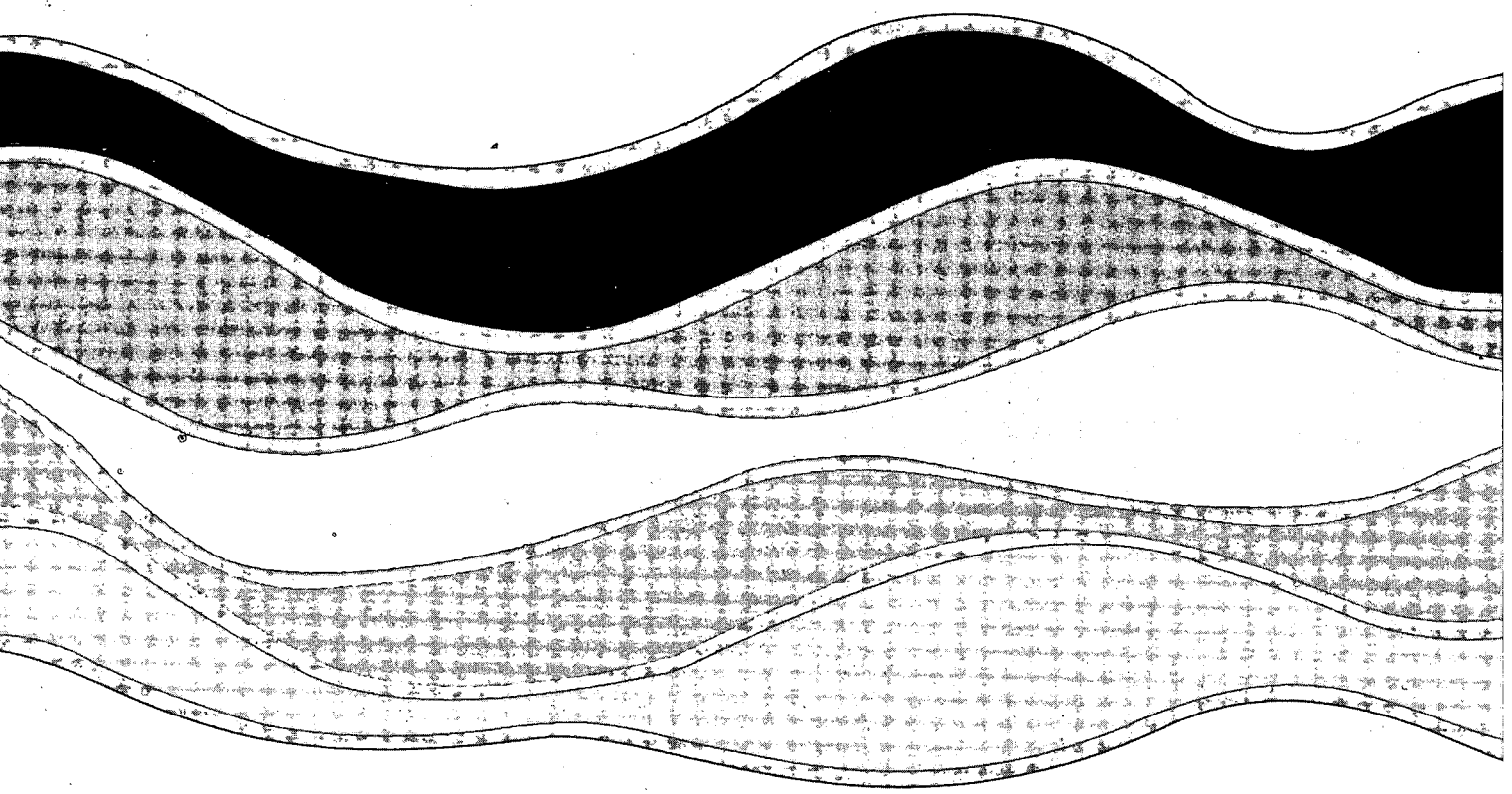

NATIONAL WATER RESEARCH INSTITUTE
P.O. BOX 5050, BURLINGTON, ONTARIO L7R 4A6

Environment Canada Environnement Canada

Canada

INSTITUT NATIONAL DE RECHERCHE SUR LES EAUX
C.P. 5050, BURLINGTON (ONTARIO) L7R 4A6

Think Recycling!

Pensez à Recycling!